Quantifying the Carboxyl Group Density of Microbial Cell Surfaces as a Function of Salinity: Insights Into Microbial Precipitation of Low-Temperature Dolomite

By

Ryan Scott Voegerl

Submitted to the graduate degree program in Geology and the Graduate Faculty of the University of Kansas in partial fulfillment of the requirements for the degree of Master of Science.

Advisory Committee

_____
Dr. Jennifer A. Roberts – Co-chair

_____
Dr. David A. Fowle – Co-chair

_____
Dr. Leigh A. Stearns

Date Defended: 5/21/2014

The Thesis Committee for Ryan S. Voegerl
certifies that this is the approved version of the following thesis:

Quantifying the Carboxyl Group Density of Microbial Cell Surfaces as a Function of Salinity: Insights Into Microbial Precipitation of Low-Temperature Dolomite

Advisory Committee

_____
Dr. Jennifer A. Roberts – Co-chair

_____
Dr. David A. Fowle – Co-chair

_____
Dr. Leigh A. Stearns

Date Approved: 5/13/2014

Abstract

Recent laboratory experiments have documented microbial mediation of low temperature dolomite precipitation via nucleation on microbial surfaces that have high (>0.06 groups $Å^{-2}$) carboxyl group densities. It is hypothesized that carboxyl groups form a cell wall complex with Mg^{2+}, dewatering the magnesium ion and overcoming kinetic barriers that allow dolomite formation at low temperature. Three microorganisms, two that precipitate dolomite in laboratory and field settings (*Desulfovibrio brasiliensis*; *Haloferax sulfurifontis*) and a control organism, not associated with dolomite precipitation (*Shewanella putrefaciens*), were selected for this research and were grown in media of varying salinities. Acid-base titrations were performed on the microorganisms, revealing an increase in buffering capacity of microorganisms grown in higher salinity growth conditions. Using ProtoFit 2.1 (Rev 1), site density values (mol/kg) were calculated for various functional groups (carboxyl, phosphoryl, and amine). For *D. brasiliensis* and *H. sulfurifontis* a 175% increase in carboxyl group density was measured (when doubling ionic strength from 0.5 M to 1.0 M) and a decrease in carboxyl group density by 47% (when reducing ionic strength from 3.2 M to 0.8 M), respectively. *S. putrefaciens*, the control specimen, also increased carboxyl group density by 70% (when increasing ionic strength from 0.1 M to 2.0 M). Calculated carboxyl group density, normalized to surface area ($Å^2$), revealed 5.56 x 10^{-1} sites $Å^{-2}$ for *D. brasiliensis* (at 1.0 M ionic strength), 1.15 x 10^{-1} sites $Å^{-2}$ for *S. putrefaciens* (at 2.0 M ionic strength), and 1.53 sites $Å^{-2}$ for *H. sulfurifontis* (at 3.2 M ionic strength), the cell wall of all three microorganisms show an increased carboxyl group density at higher salinities, and a lower carboxyl group density when grown at lower salinities. These data demonstrate that increases of carboxyl group density are evidence for environmental control on microorganisms. Microorganisms respond to increasing salinities by modifying their exterior cell wall as a coping mechanism to high ionic strength and osmotic pressure. Under these conditions, typical of mixing zones of fresh and marine waters, sabkha and hypersaline lagoon environments, microbial cell walls may serve as nucleation sites for low temperature dolomite when geochemical conditions for dolomite are favored.

Acknowledgments

Dr. Jennifer Roberts, from the day we met, you have been my lifeboat in graduate school. I could not have wished for a better research advisor and colleague. Your patience and endurance are truly remarkable. The University of Kansas is a better place, because of you.

Dr. David Fowle, your microbial knowledge and professional advice is both wide and deep. Please continue to expand your research to distant, unknown horizons.

Dr. Leigh Stearns, thank you for advice and assistance with my thesis work.

Dr. Masato Ueshima, Dr. Karla Leslie, Christa Jackson, Josh Boling, & Greg Cane, thank you for laboratory assistance and advice.

The Kansas Interdisciplinary Carbonate Consortium has provided research funding for this project. Thank you for your contributions to this research.

My wife, Erica, thank you for being my best friend and companion. Graduate school was easier with your constant feedback and inspiration. Also, your back rubs are amazing.

Table of Contents

Chapter 1: Introduction

Overview

Dolomite [$CaMg(CO_3)_2$], a carbonate mineral, is found in abundance within the rock record, but forms scarcely in modern environments (Vasconcelos and McKenzie, 1997). Understanding the relative scarcity of dolomite in modern environments is due to a lack of secondary dolomite, e.g. active dolomitization of limestone by Mg-rich fluids (McKenzie & Vasconcelos, 2009), but also by a significant kinetic barrier to primary dolomite precipitation at low temperature (<50 °C), confounding its laboratory synthesis (Land, 1998). Much of the laboratory synthesis of dolomite at low-temperature has produced negative results (e.g., Braithwaite et al., 2004; McKenzie, 1991), leading geoscientists to consider parameters other than purely abiotic components that may play a role in low temperature dolomite nucleation and precipitation (Vasconcelos and McKenzie, 1997).

Recent biotic models and experimentation, that includes microorganisms and their exudates, have demonstrated that dolomite precipitation is possible at low temperatures (<50°C) in laboratory settings, by microbial influence and mediation (e.g., Vasconcelos et al., 1995; Roberts et al., 2004; Mastandrea et al., 2006; Sánchez-Román et al., 2008; Kenward et al., 2013). Many of these studies have observed dolomite precipitates that are intimately associated with microbial surfaces (Warthmann et al., 2000; van Lith et al., 2003) and recent studies have implicated microbial exopolymeric substances (Rivadeneyra et al., 1996; Dupraz et al., 2004; Sánchez-Román et al., 2007) in its formation (Krause et al. 2012).

Dolomite Formation in Modern Low-Temperature Environments

Modern precipitation of dolomite has been documented in various locations around the world. One prominent research location is found in the coastal hypersaline lagoon "*Lagoa Vermelha*" (Portuguese for "Red Lagoon"), found 90 kilometers east of Rio de Janeiro, Brazil (Vasconcelos and McKenzie, 1997). Weakly-lithified dolomite concretions have been collected from the lagoon, from an anoxic "black sludge" layer (10-14 cm depth). Between depths of 20-40 cm, aggregates of triangular prisms of dolomite appear to diverge from a common nucleus, while other crystals form a radial aggregate dolomite structure with twisted interlocking semi-dumbbells. At depths of 70 cm, well-developed euhedral crystals of dolomite have also been collected.

The formation of these dolomite crystals has been linked to interactions with sulfate-reducing bacteria found in the lagoon. The salinity of Lagoa Vermelha is supported by a delicate balance of freshwater input, via wet season precipitation, and marine water influx via landward percolation, during the dry season. The continuous input and recirculation of dissolved ions (Ca^{2+}, Mg^{2+}, CO_3^{2-}, SO_4^{2-}) provide the necessary chemical mix for dolomite precipitation to occur (with SO_4^{2-} serving as the terminal electron acceptor for metabolic activity of sulfate-reducing bacteria). One isolated strain of sulfate-reducing bacteria, *Desulfovibrio brasiliensis*, later became the central focus of dolomite precipitation in Lagoa Vermelha.

Another area of modern dolomite precipitation is found in distal ephemeral lakes of the Coorong region of South Australia (Wright, 1999). This region of Australia has a climate conducive to dolomite precipitation, with salinity increases during the late spring/summer

driven by increased rates of evaporation with decreased rates of freshwater recharge. The dolomite found in this area has been determined to be recent, with radiocarbon dating giving results to an age of 300 ± 250 years. The dolomite is primary (precipitated *in situ*), and evidence for secondary replacement (dolomitization) is absent. No dolomite is found in nearby interdune flats or calcareous dunes, and therefore, related solution chemistry favoring dolomite precipitation is found in the immediate area. Similar to conditions described in Brazil, a variety in seasonal evaporation maintains high salinity values within the lake. In this case, local sulfate-reducing bacteria have also been linked to dolomite precipitation, in the form of aggregations of submicron-sized dolomite sediments. The dolomite grains are subspherical/elliptical in morphology, with a "bacterial-shaped" core, covered with a overgrowth of white dolomite. These grains are interpreted to be dolomite-encapsulated bacterial cells.

The Role of Cell Wall Functional Groups

In addition to linkages between low temperature dolomite formation and different microbial metabolism, such as sulfate reducers, methanogens, methanotrophs, aerobic heterotrophs and sulfide oxidizers, many of these reports also include observations of dolomite in close proximity to microbial surfaces or exopolysaccharides (EPS; van Lith et al., 2003, Roberts et al., 2013, Kenward et al., 2013, Braissant et al., 2007, etc.). Despite these reports of involvement of microbial surfaces in low temperature dolomite formation, specific mechanisms have remained elusive until recent work by Kenward et al. (2013) and Roberts et al. (2013) demonstrated that microbial cells with relatively high densities of carboxyl groups (>0.06

groups Ångstrom^{-2}) and carboxylated organic matter promote dolomite formation at laboratory temperatures of 25°C.

A relatively high abundance of carboxyl groups (R-COOH) is present on bacterial cell wall surfaces, in comparison with other functional groups. When found in circum-neutral pH (6.0-8.0), most carboxyl groups are found in a deprotonated state (-), allowing positively-charged cations, such as magnesium, to be attracted to the negatively-charged functional groups. Solutions that contain high concentrations of dissolved ions (e.g., magnesium, sodium, chloride) have an increased probability of chemical interaction between dissolved metals and ligands, such as carboxyl groups.

As a solution's pH becomes more alkaline, passing the pKa value (50% deprotonation) for various functional groups (carboxyl, phosphoryl, and amine), a transition to complete deprotonation occurs. However, the range for pKa values are unique for each functional group. Previous titration experiments by Haas et al. (2001) with *Shewanella putrefaciens* demonstrate distinct deprotonation ranges of functional groups, progressing from carboxyl to phosphoryl and ending with amine groups. The determined pKa values for *Shewanella putrefaciens* were 5.16 ± 0.04 for carboxyl, 7.22 ± 0.15 for phosphoryl, and 10.04 ± 0.67 for amine groups. These distinct ranges of deprotonation allow comparative study of carboxyl group density of the cell wall of microorganisms.

Many microbial cell wall surfaces have been characterized but few, if any, organisms from dolomite-forming environments have been characterized. However, recent work (Kinnebrew, 2012) suggests that archaean cells grown under high dissolved ion concentrations could promote a relatively high density of cell wall functional groups, including carboxyl groups.

These surface-bound carboxyl groups ($R\text{-}COO^-$) serve as potential binding sites for cations, initiating surface complexation between Mg^{2+} and carboxyl groups (Kenward, 2013). Dissolved Mg^{2+} ions are covered by a "hydration sphere" of six molecules of water, creating a kinetic barrier around the magnesium ion. As the magnesium-carboxyl group complex forms, a dehydration reaction occurs, and one of the initial six water molecules surrounding the Mg^{2+} ions is ejected into solution. This reaction is energetically favorable, as the difference in Gibb's free energy is 13.6 kcal mol^{-1} lower (Katz, 1996).

$Mg(H_2O)_6]^{2+} + R\text{-}COO^- \rightarrow [Mg(H_2O)_5(R\text{-}COO)]^+$ (ΔH = -199.8 kcal mol^{-1})

Following the formation of the magnesium-carboxyl complex, a carbonate ion (CO_3^{2-}) may bind to the magnesium ion, creating a template for subsequent binding of Ca^{2+} and CO_3^{2-}, a thin layer of dolomite. Experimental research has determined that microorganisms and natural organic matter with a high density of surface-bound carboxyl groups (>0.06 groups $Å^{-2}$) readily bind Mg^{2+} ions, facilitating a template for dolomite precipitation (Roberts et al., 2013; Kenward et al., 2013). After growing in increased ionic strength conditions, multiple microorganisms have been documented to increase apparent total site (functional group) densities (Borrok et al, 2005). Modification of the cell wall is a direct response to an increase in salinity, possibly as a survival mechanism.

The goal of this research project is to test the following hypothesis: **The density of surface-bound carboxyl groups in microorganisms is, in part, controlled by salinity, with increasing densities at higher salinity (>50 ‰) and lower densities at lower salinities (<30 ‰).** It follows then, that microbial biomass in hypersaline or slightly evaporated marine

environments may serve as effective nucleation sites for the formation of dolomite (e.g. Roberts et al., 2013).

References

Borrok, D., Turner, B. F., & Fein, J. B., 2005, A universal surface complexation framework for modeling proton binding onto bacterial surfaces in geologic settings. *American Journal of Science*, v. 305, n. 6, p. 826-853.

Braithwaite, C. J., Rizzi, G., & Darke, G., 2004, The geometry and petrogenesis of dolomite hydrocarbon reservoirs: introduction. *Geological Society, London, Special Publications*, v. 235, n. 1, p. 1-6.

Braissant, O., Decho, A. W., Dupraz, C., Glunk, C., Przekop, K. M., & Visscher, P. T., 2007, Exopolymeric substances of sulfate-reducing bacteria: Interactions with calcium at alkaline pH and implication for formation of carbonate minerals, *Geobiology*, v. 5, n. 4, p. 401-411.

Dupraz, C., Visscher, P.T., Baumgartner, L.K., and Reid, R.P., 2004, Microbe-mineral interactions: Early carbonate precipitation in a hypersaline lake (Eleuthera Island, Bahamas), *Sedimentology*, v. 51, p. 745–765.

Haas, J. R., Dichristina, T. J., & Wade, R., 2001, Thermodynamics of U (VI) sorption onto *Shewanella putrefaciens, Chemical Geology*, v. 180, p. 33-54.

Katz, A. K., Glusker, J. P., Beebe, S. A., & Bock, C. W., 1996, Calcium ion coordination: a comparison with that of beryllium, magnesium, and zinc. Journal of the American Chemical Society, v. 118, n. 24, p. 5752-5763.

Kenward, P. A., Fowle, D. A., Goldstein, R. H., Ueshima, M., Gonzalez, L. A., & Roberts, J. A., 2013, Ordered low-temperature dolomite mediated by carboxyl-group density of microbial cell walls. *AAPG Bulletin*, v. 97, n. 11, p. 2113-2125.

Kinnebrew, N., 2012, Surface Sorption Properties of Halophilic Archaea, University of Kansas Master's Thesis, p. 1-55.

Krause, S., Liebetrau, V., Gorb, S., Sánchez-Román, M., McKenzie, J. A., & Treude, T., 2012, Microbial nucleation of Mg-rich dolomite in exopolymeric substances under anoxic modern seawater salinity: New insight into an old enigma: *Geology*, v. 40, p. 587-590.

Land, L. S., 1998, Failure to Precipitate Dolomite at 25° C from Dilute Solution Despite 1000-Fold Oversaturation after 32 Years. *Aquatic Geochemistry*, v. 4, n. 3, p. 361-368.

Mastandrea, A., Perri, E., Russo, F., Spadafora, A., Tucker, M., 2006, Microbial primary dolomite from a Norian carbonate platform: northern Calabria, southern Italy: *Sedimentology*, v. 53, p. 465–480.

McKenzie, J. A., Vasconcelos, C., 2009, Dolomite Mountains and the origin of the dolomite rock of which they mainly consist: historical developments and new perspectives. Sedimentology, v. 56, n. 1, p. 205-219.

McKenzie, J.A., 1991, The dolomite problem: An outstanding controversy, *in* Müller,D.W., et al., eds., Controversies in modern geology: Evolution of geological theories in sedimentology, Earth history and tectonics: London, Academic Press, p. 37-54.

Müller DW, McKenzie JA, Mueller PA, 1990, Abu Dhabi sabkha Persian Gulf revisited: application of strontium isotopes to test an early dolomitization model: *Geology,* v. 18, p. 618–621.

Rivadeneyra, M.A., Ramos-Cormenzana, A., Delgado, G., and Delgado, R., 1996, Process of carbonate precipitation by *Deleya halophila*: *Current Microbiology*, v. 32, p. 308–313.

Roberts, J. A., Kenward, P. A., Fowle, D. A., Goldstein, R. H., González, L. A., & Moore, D. S., 2013, Surface chemistry allows for abiotic precipitation of dolomite at low temperature, *Proceedings of the National Academy of Sciences*. v. 110, n. 36, p. 14540-14545.

Roberts, J.A., Bennett, P.C., Gonzalez, L.A., Macpherson, G.L., Milliken, K.L., 2004, Microbial precipitation of dolomite in methanogenic groundwater: *Geology*, v. 32, p. 277–280.

Sánchez-Román, M., Vasconcelos, C., Schmid, T., Dittrich, M., McKenzie, J.A., Zenobi, R., Rivadeneyra, M.A., 2008, Aerobic microbial dolomite at the nanometer scale: implications for the geologic record, *Geology*, v. 36, p. 879–882.

Sánchez-Román, M., Rivadeneyra, M., Vasconcelos, C., McKenzie, J.A., 2007, Biomineralization of carbonate and phosphate by halophilic bacteria: Influence of Ca^{2+} and Mg^{2+} ions, *FEMS Microbiology Ecology*, v. 61, p. 273–284.

Sokolov, I., Smith, D.S., Henderson, G.S., Gorby, Y.A., Ferris, F.G., 2001, Cell surface electrochemical heterogeneity of the Fe(III)-reducing bacteria Shewanella putrefaciens. *Environmental Science &Technology,* v. 36, p. 341–347.

Turner, B. F., & Fein, J. B., 2006, Protofit: a program for determining surface protonation constants from titration data. Computers & geosciences, v. 32, n. 9, p. 1344-1356.

Vasconcelos, C. and McKenzie, J.A., 1997, Microbial mediation of modern dolomite precipitation and diagenesis under anoxic conditions (Lagoa Vermelha, Rio de Janeiro, Brazil). J. Sediment. Res., v. 67, p. 378–390.

Vasconcelos, C., McKenzie, J. A., Bernasconi, S., Grujic, D., & Tiens, A. J., 1995, Microbial mediation as a possible mechanism for natural dolomite formation at low temperatures. Nature, v. 377, n. 6546, p. 220-222.

van Lith, Y., Warthmann, R., Vasconcelos, C., & McKenzie, J. A., 2003, Microbial fossilization in carbonate sediments: a result of the bacterial surface involvement in dolomite precipitation, *Sedimentology*, v. 50, p. 237-245.

Warthmann, R., van Lith, Y., Vasconcelos, C., McKenzie, J., Karpoff, A.M., 2000, Bacterially induced dolomite precipitation in anoxic culture experiments, Geology, v. 28, p. 1091-1094.

Wright, D. T., 1999, The role of sulphate-reducing bacteria and cyanobacteria in dolomite formation in distal ephemeral lakes of the Coorong region, South Australia. Sedimentary Geology, v. 126, n. 1, p. 147-157.

Chapter 2: Quantifying Carboxyl Group Density Via Titration

Introduction

The exterior cell walls of microorganisms host a variety of functional groups (e.g. carboxyl, phosphoryl, amine) (Figure 1), allowing each cell to interact with its surrounding environment by chemical and electrostatic interactions with dissolved ions (e.g. cadmium, copper, lead, aluminum, magnesium; Fein et al., 1997). Understanding how these surface-bound functional groups specifically interact with these ions, can provide insight into metal toxicity, metabolic uptake, and biomineralization by microorganisms (Daughney et al., 1998). Therefore, it is of critical importance to develop mechanistic models to quantify ion interaction with cell surfaces. Borrok et al. (2005) have created a universal surface complexation framework model that has determined pKa values of 3.1, 4.7, 6.6, and 9.0 for cell wall functional groups (as phosphodiester, carboxyl, phosphoryl, amine, respectively). When in a deprotonated state, these functional groups can potentially create bonds with dissolved cations, allowing such microorganisms to be used in bioremediation efforts of metal contaminants (Gadd, 2004). When microorganisms are grown in harsh, dynamic salinity fluxes, as seen in: mixing zones in sabkha environments of the Persian Gulf (Müller, et al., 1990), hypersaline lagoons of Brazil (Warthmann et al., 2000), and the Coorong lakes of Australia (Warren, 1990), the total site (functional group) density can increase (Borrok et al., 2005). When grown in stressful environmental conditions, microorganisms may exhibit cell wall thickening, a modification that increases survival probability (Cunningham & Spreadbury, 1998; Van Houte & Saxton, 1971; Shockman, 1965). Thickened cell walls can offer protection from

increased osmotic pressures, by increasing cell wall rigidity, as experienced in hypersaline conditions.

A series of acid-base titration experiments can be used to test functional group density of the cell wall, by observing an increased buffering capacity for microorganisms resulting from increased functional group density. An increased buffering capacity is observed when an increased amount of acid or base is necessary to titrate to reach a desired pH endpoint. The buffering capacity of a microorganism increases as an increased functional group density readily binds with free ions of H^+.

This research aims to grow three microorganisms in a variety of solution salinities and measure any response cells may have in adapting to changes in salinity by changing functional group density (Borrok et al., 2005) of the exterior cell wall.

Methods

Three microorganisms, two that have been shown to precipitate dolomite in laboratory and field settings at a range of salinities (*Desulfovibrio brasiliensis*; *Haloferax sulfurifontis*) and a control organism, that has not previously been associated with dolomite precipitation (*Shewanella putrefaciens*), were selected for this research (Table 1).

The bacterial species *Desulfovibrio brasiliensis* strain LVform1 (DSMZ; DSM# 15816), known to precipitate dolomite crystals in the hypersaline lagoon, Lagoa Vermelha (Brazil), acquired from the DSMZ (Deutsche Sammlung Mikroorganismen Zellkulturen), were cultured under anaerobic conditions in 10 mL batches in 15 mL Hungate tubes using 0.5 M ionic strength DSMZ recipe Medium 383 (Table 2) and incubated at 30°C on a rotisserie at 8 rpm.

The bacterial species *Shewanella putrefaciens* strain 200R (ATCC® 51753™), acquired from ATCC (American Type Culture Collection), a well studied microorganism that has not been implicated in dolomite precipitation (Kenward et al., 2013), is a facultative anaerobe, isolated from an oil pipeline in Alberta, Canada. The bacteria were cultured under aerobic conditions in 10 mL batches in 15 mL Falcon tubes of BD™ Trypticase™ soy broth (calculated initial ionic strength of 0.1 and additional ionic strength increases by addition of NaCl), and incubated at 30°C in an agitating incubator at 170 rpm.

The archaeal species *Haloferax sulfurifontis* strain M6 (DSMZ; DSM# 16227) was acquired from DSMZ. It is known to precipitate dolomite crystals under laboratory conditions (e.g. Kenward et al., 2013) and was isolated from a southwestern Oklahoma spring (rich in both sulfide and sulfur ions). It was cultured under aerobic conditions in 10 mL batches in 15 mL Falcon tubes of ATCC® Medium 2448, yeast extract medium (original ionic strength 3.2 M), and incubated at 37°C in an agitating incubator at 170 rpm.

Media were prepared with deionized water (18MΩ) by process of reverse osmosis. All prepared media solutions were autoclaved for 30 minutes at 121°C. Growth curves were generated by completing cell counts (e.g. Yu et al., 1995) after the following time intervals: *D. brasiliensis* reached mid-exponential growth phase after 2.0-2.5 days of incubation (Figure 2), *S. putrefaciens* after 4-5 hours (Figure 3), and *H. sulfurifontis* after 6-8 hours (Figure 4). These times were used for the incubation period for harvesting and titration.

Each microorganism was grown in various ionic strength medium solutions (Table 5) by creating calculated changes in concentrations of medium reagents: increased and decreased proportioned amounts of reagents listed under "Solution A" for *Desulfovibrio brasiliensis* (Table

2), NaCl concentrations for *Shewanella putrefaciens* (Table 3), and NaCl concentrations for *Haloferax sulfurifontis* (Table 4). *D. brasiliensis* was grown in ionic strength conditions that were higher (up to 1.5 M ionic strength) and lower (down to 0.2 M ionic strength) than optimal growth conditions (original 0.5 M ionic strength). *S. putrefaciens* was grown in higher ionic strengths (up to 3.0 M ionic strength) compared to optimal medium conditions (original 0.1 M ionic strength). *H. sulfurifontis* was grown in lower ionic strengths (down to 0.2 M ionic strength) from optimal growth conditions (original 3.2 M ionic strength). Microorganisms experienced three generations (and ten generations) growth time in their selected ionic strength medium before being harvested for titration experimentation.

Microorganisms were grown to mid-exponential phase, harvested and centrifuged into pellets at 3,750 rpm for 15 minutes. Pellets were reduced to a wet mass of 0.05 g, and rinsed (5x) with 50 mL 0.1 M NaCl solution. The 0.1 M NaCl solution was previously bubbled with N_2 gas for one hour, to remove any dissolved CO_2. Titrations were performed using Tiamo® Titration hardware (Metrohm Titrando 842 autotitrator) and associated software created by Metrohm USA Inc. Microbial pellets submerged in 50 mL 0.1 M NaCl solutions were titrated down to pH 3.2 (0.1 M HCl), up to pH 8.0 (0.1 M NaOH), and again down to pH 3.2. Laboratory temperatures, during titrations, were 22±1°C. Raw titration data (pH levels and acid/base added) and associated curves were exported from output reports (Turner & Fein, 2006).

Titration data, including: acid/base added (mL), pH changes, initial temperature, pellet mass, specific surface area of absorbent, and the number of titration steps, was input and evaluated by ProtoFit software 2.1 Rev1 (Turner and Fein, 2006). Analysis by ProtoFit generated estimated pK_a values (acid dissociation constants) for various functional groups

(carboxyl, phosphoryl, amine) found on the cell wall exterior of the microorganisms studied. Functional group concentrations were calculated in units of "moles of functional group per kilogram" of microorganism (mol/kg), and then converted for easy comparison. Example: Site density of log C -1.00 converts to $10^{-1.00}$ which equals 0.1 moles of functional group sites per kilogram (mol/kg) of microorganism.

Calculations of high, medium, and low surface areas were completed for each of the microorganisms by using measurements of length and width (Warthmann, 2005; Sokolov et al., 2001; Elshahed, et al., 2004). Carboxyl group density per $Å^2$ was calculated and compared among the microorganisms.

Results

Titrations

All titration data was exported from the Tiamo® Titration software and plotted for comparison purposes. Acid titrations for *D. brasiliensis* were compared to a mean pKa curve with mean site densities, to show reproducibility (Figure 5). Titration data was also plotted showing differences in cell wall buffering capacity between *D. brasiliensis* and *H. sulfurifontis*, depending on ionic strength growth conditions (Figure 6). *D. brasiliensis* required 0.50 mL of acid to reach the titration goal (pH 3.2), during 0.5 M ionic strength growth conditions (Figure 6A). However, when *D. brasiliensis* was grown in increased ionic strength conditions (1.5 M), 0.77 mL of acid was required to reach the titration goal (pH 3.2), an acid increase of 53.7%. During optimal (0.1 M) ionic strength growth conditions *S. putrefaciens* required 0.69 mL of acid to reach the titration goal (pH 3.2), with other trials within a similar range (Figure 6B). During optimal (3.2 M) ionic strength conditions, *H. sulfurifontis* required 0.75 mL of acid to reach the

titration goal (down to pH 3.2) (Figure 6C), and only needed 0.48 mL of acid when grown in a reduced ionic strength of 0.2 M; a decrease in acid by 36.2%.

ProtoFit Analysis Results

All titration data was input into ProtoFit 2.1 (Rev 1; Turner and Fein, 2006), and analyzed to calculate the acid dissociation constants (pK_a values) and site density (mol/kg). Analysis by ProtoFit 2.1 revealed increased carboxyl group densities for all three microorganisms after multi-generational growth in higher salinity conditions (Table 6).

Desulfovibrio brasiliensis

Initial site density of carboxyl groups was measured to be 0.09 (± 0.01) mol/kg. After growing *D. brasiliensis* in ionic strength conditions of 1.0 M, the carboxyl group density increased by 189% to 0.26 (± 0.01) mol/kg. Total site density measurements followed a similar trend from 0.27 (± 0.02) mol/kg to 0.60 (± 0.07) mol/kg, an increase of 122%. These changes in functional group density occurred within three generations of growth in increased ionic strength conditions. Measurements were taken after ten generations of growth with similar results (Figure 7). Averaged values from low ionic strength conditions (0.2-0.5 M), 1.0 M, and 1.5 M ionic strength conditions have also been summarized (Figure 8).

Shewanella putrefaciens

Initial site density of carboxyl groups was measured to be 0.13 (± 0.01) mol/kg. After growing *S. putrefaciens* in ionic strength conditions of 2.0 M, the carboxyl group density

increased by 69% to 0.22 (± 0.02) mol/kg. Total site density measurements showed another increasing trend from 0.88 (± 0.06) mol/kg to 1.1 (± 0.1) mol/kg, an increase of 25%. Measurements of carboxyl group density after three generations displayed an overall decrease in total site density, followed by an increasing rebound in total site density after ten generations (Figure 9). Averaged values from initial conditions (0.1 M ionic strength), 1.0-3.0 M ionic strength (three generations), and 1.0-3.0 M ionic strength (ten generations) conditions have also been summarized (Figure 10).

Haloferax sulfurifontis

Initial site density of carboxyl groups was measured to be 0.34 (± 0.04) mol/kg. After growing *H. sulfurifontis* in decreased ionic strength conditions of 1.0-0.2 M, the carboxyl group density decreased by 47% to 0.18 (± 0.04) mol/kg. Total site density measurements also decreased from 0.77 (± 0.11) mol/kg to 0.60 (± 0.15) mol/kg, a decrease of 22%. These measured changes in functional group density were all taken after three generations of growing in decreased ionic strength conditions (Figure 11). Averaged values from low ionic strength conditions (0.2-0.5 M), 1.0 M, and 1.5 M ionic strength conditions have also been summarized (Figure 8).

Carboxyl Group Density per Å^2

Carboxyl group density values were converted to carboxyl site density per Å^2. At optimal growth conditions (0.5 M ionic strength) *D. brasiliensis* had an initial carboxyl group density of 2.02 x 10^{-1} sites Å^{-2}, and after growth in experimental ionic strength media (1.0 M), the carboxyl group density increased to 5.56 x 10^{-1} sites Å^{-2}. At optimal growth conditions (0.1

M ionic strength) *S. putrefaciens* had an initial carboxyl group density of 6.76 x 10^{-2} sites $Å^{-2}$, and after growth in experimental ionic strength media (2.0 M), the carboxyl group density increased to 1.15 x 10^{-1} sites $Å^{-2}$. At optimal growth conditions (3.2 M ionic strength), *H. sulfurifontis* had an initial carboxyl group density of 1.53 sites $Å^{-2}$, and after growth in experimental ionic strength media (0.4-0.8 M), the carboxyl group density decreased to 8.07 x 10^{-1} sites $Å^{-2}$. Calculated surface areas are displayed for each microorganism (Table 7). Initial carboxyl group density per $Å^2$ was calculated and compared with the carboxyl group density of the experimental batch trials (Figure 13).

Discussion

Desulfovibrio brasiliensis

Desulfovibrio brasiliensis (strain LVform1) was isolated from the hypersaline lagoon "Lagoa Vermelha" near Rio de Janeiro, Brazil (Figure 14) (22°55'50"S, 42°23'40"W). This hypersaline lagoon experiences greater rates of evaporation than precipitation for ten months of the year (Figure 15), creating high salinity conditions that support various microbial communities (Vasconcelos and McKenzie, 1997). Wet season conditions create an influx of freshwater that temporarily produce brackish conditions, followed by a dry season, returning conditions to saline conditions. After several months of intense evaporation, the salinity values (ionic strength) of the lagoon are great enough to be considered hypersaline (>3.5% dissolved mineral salts; >0.72 M ionic strength).

However, daily rainfall during the wet season, or a landward influx of seawater (storm surge) could influence salinity changes on a daily basis. Microorganisms of the lagoon would require cell wall modification mechanisms, as described in this research, to survive the flux in

salinity. These mechanisms may increase the probability of dolomite precipitation by increasing the associated carboxyl group density found on the exterior cell wall.

Research completed by Warthmann et al. (2005) has shown field precipitation of dumbbell-shaped dolomite minerals occurs within Lagoa Vermelha, however, these findings do not elaborate on the live/dead status of *D. brasiliensis* at the time of crystal development. Complete dolomite crystal encapsulation is also ambiguous, and can be assumed, but conclusive evidence is currently absent. Phoenix et al. (2002) suggest that bacterial sheaths, similar to dolomite precipitation, might be loosely bound to the cell surface, easily sloughed off, by breaking weak bonds between the sheath and the bacterial cell wall. Another study suggests that the sloughing of cyanobacteria sheaths may provide a protective mechanism against biomineralization, specifically silicification of the cell wall (Phoenix et al., 2000). The dolomite template formed on the cell wall of *D. brasiliensis* may serve as a protective mechanism from temporary inhospitable conditions, that may also be sloughed off when conditions are favorable for survival (lower salinities). Upon cellular death, perhaps complete encapsulation (Warthmann's "Dolomite Dumbbell") of the dolomite template may be complete, as the bacteria is unable to slough off the dolomite crystals. Alternatively, Kenward et al. (2013) demonstrated that only dead or non-metabolizing cells precipitated dolomite under laboratory conditions, therefore encapsulation during precipitation may only occur on dead biomass.

When examining Lagoa Vermelha environmental data collected by Vasconcelos and McKenzie, seasonal temperatures vary between 23-32°C and the pH range is well buffered between 8.0-8.5 (Table 8). Magnesium to calcium ratios range from 1.66-3.17, throughout the

year. During the dry season, from April through June, environmental conditions become ideal (e.g. high ionic strength, low Mg:Ca ratio) for microbial dolomite precipitation and therefore low temperature dolomite formation requires both favorable geochemical conditions as well as appropriate microbial biomass to serve as nucleation surfaces. These requirements may also be present in other geologic environments that support high salinity fluxes (hypersaline lagoons of Brazil, Coorong lakes of Australia, and mixing zones of sabkha of the Persian Gulf) have documented modern dolomite precipitation (Müller, et al., 1990; Warthmann et al., 2000; Warren, 1990).

This strain of *Desulfovibrio brasiliensis* (LVform1) survives in dynamic salinity conditions, both on a daily and seasonal basis, and displays rapid exterior cell wall modification (three generations) as a means of adaptation and proliferation. This accelerated method of adaptation not only increases survival probability, but also increases probability of dolomite precipitation.

Roberts et al. (2013) describes the carboxyl group density for the average bacteria to be 6.0×10^{-2} sites $Å^{-2}$ on the exterior cell wall. Kenward et al. (2013) describes a dolomite precipitation threshold value to be greater than, or equal to, 0.06 sites $Å^{-2}$ (Table 9). The initial carboxyl group density measurement, taken after growth in optimal ionic strength, of *D. brasiliensis* was 2.02×10^{-1} sites $Å^{-2}$, and after growth in twice the ionic strength (0.5 to 1.0), the carboxyl group density increased by 175% to 5.56×10^{-1} sites $Å^{-2}$. Both low ionic strength (0.5 M) and high ionic strength conditions (1.0 M) produced carboxyl group density values ($Å^{-2}$) above the threshold value of >0.06 sites $Å^{-2}$. High ionic strength conditions increased the

carboxyl group density ($Å^{-2}$) and ultimately increases the probability for the dehydration of Mg^{2+}, a key step in the precipitation of dolomite, as described by Roberts et al. (2013).

Shewanella putrefaciens

Shewanella putrefaciens (strain 200R) was isolated from an oil pipeline in Alberta, Canada (Obuekwe, 1980). Environmental conditions of the oil pipeline have subjected *S. putrefaciens* to a wide range in salinity and pH, driving cell wall adaptations to occur. However, these conditions found in the pipeline, relatively consistent in the short term, allow *S. putrefaciens* to adapt to fluxes in salinity but at a much slower rate than bacteria that experience great fluxes in salinity changes on a daily basis (*D. brasiliensis*).

In this study, *S. putrefaciens* responded to increases in ionic strength, however, at a much slower rate of cell wall modification, when compared to *D. brasiliensis*. *S. putrefaciens* required at least four generations to begin adaptation to increased ionic strengths, with a net result of increased carboxyl group density and total site density after ten generations of growth. The measured initial carboxyl group density 6.76 x 10^{-2} sites $Å^{-2}$ is slightly greater than the average bacterial carboxyl group density of 6.0 x 10^{-2} sites $Å^{-2}$ (Roberts et al., 2013). After ten generations of growth in 2.0 ionic strength, *S. putrefaciens* increased the carboxyl group density to 1.15 x 10^{-1} sites $Å^{-2}$, an increase of 70%.

Multigenerational adaptation (e.g. cell wall thickening/increased functional groups) occurs after successive negative environmental conditions continuously threaten the survival of the microorganism. Each successive generation of *S. putrefaciens* survived the subsequent increase in salinity by cell wall modification, by increasing cell wall components and functional

groups. *S. putrefaciens* is not currently associated with dolomite precipitation, however, future experimentation could show otherwise.

Haloferax sulfurifontis

Haloferax sulfurifontis (strain M6) was isolated from a microbial mat from a sulfur spring in Oklahoma, United States of America. Members of the archaean domain are known for their incredible resiliency to thrive in inhospitable environments, and *H. sulfurifontis* is no exception. *H. sulfurifontis* optimally grows in high ionic strength conditions (3.2 M initial ionic strength) and adapts quickly (three generations) to decreased ionic strength conditions, however potentially shedding its surficial S-layer.

H. sulfurifontis possesses an S-layer that provides reinforcement and rigidity to the cell exterior (Sára & Sleytr, 2000), as well as allowing protection from the environment and other microorganisms (Beveridge & Graham, 1991). As the S-layer can provide protection from harsh environmental conditions, perhaps the S-layer was shed as ionic strength was reduced throughout the duration of the experimental trials, and as a result, any carboxyl groups that were bound to the S-layer were also lost. A color change was noted between 1.6-1.0 M ionic strength from dark red to light peach coloration, possibly as a loss of the S-layer (surface protein layer) found on the cell wall.

The measured initial carboxyl group density 1.53 sites $Å^{-2}$ places *H. sulfurifontis* into the high probability category for dolomite precipitation to occur. After decreasing ionic strength to 0.8 M, the carboxyl group density also decreased to 8.07 x 10^{-1} sites $Å^{-2}$, a decrease of 47%.

Research completed by Kenward et al. (2013) has shown that ordered dolomite can be

precipitated by non-metabolizing cells of *H. sulfurifontis*, while supersaturated solutions did not produce dolomite in the absence of *H. sulfurifontis* cell material. The carboxyl group covered archaeal biomass is thought to have overcome the kinetic barrier of the hydration sphere surrounding the free Mg^{2+} ions, as the proposed mechanism that serves as the initial step of creating a dolomite template (Figure 16).

H. sulfurifontis research completed by Kinnebrew (2012) has correlated high site densities with high ionic strengths, which is in accordance with research described in this thesis (Figure 17). Kinnebrew has demonstrated that adsorption reactions, the binding of free cations (hydrogen and lead) onto the exterior cell surface of *H. sulfurifontis*, occur readily and are reversible among the functional group sites of the cell surface. Kinnebrew suggests that this adaptation is a passive protection mechanism against heavy metal cations (e.g. Pb^{2+}, Cd^{2+}) of the surrounding environment.

Research completed by Dawson et al. (2012) analyzed cell wall lipids of archaeans with different salinity tolerances has demonstrated that dialkyl glycerol diether compounds (location where functional groups bind on the cell wall) increase when archaeans are grown in higher salinity conditions, consistent with the results from this study. The fraction of unsaturated dialkyl glycerol diether compounds of *Halorhabdus utahensis*, *Natronomonas pharaonis*, *Haloferax sulfurifontis*, and *Halobaculum gomorrense* show a distinct increasing trend when plotted against optimal salinity growth strength (Figure 18), suggesting that archaeans (*H. utahensis*, *N. pharaonis*) may have even greater functional group densities than examined in this research.

Additional Mechanisms for Surviving Osmotic Stresses

Microorganisms that flourish in hypersaline conditions must find ways to survive the high osmotic stresses (water moving from the cell interior to create equilibrium with the environment exterior) that is experienced in high salinity conditions. Microorganisms have two options to create "osmotic equilibrium" within and around the cells: (1) cells may maintain high intracellular salt concentrations (the "salt-in" strategy) or (2) cells may maintain minimal salt concentrations within the cytoplasm, and instead, store organic solutes within the cytoplasm (the "compatible-solute" strategy) (Oren, 1999). Many halophilic archaeans take in KCl, while excluding Na^+ (solution 1), and conversely, eukaryotes and halophilic bacteria survive by intake and storage of organic solutes (solution 2) (Dawson et al., 2012).

Conclusions

Environmental salinity conditions influence microbial cell wall modification by increasing or decreasing functional group density within ten growth generations. *Desulfovibrio brasiliensis* increases carboxyl group density by 175%, when grown in increased (2x) ionic strength salinity conditions. *Shewanella putrefaciens* increases carboxyl group density by 70%, when grown in increased (20x) ionic strength salinity conditions. Conversely, *Haloferax sulfurifontis* can decrease carboxyl group density by 47% when grown in decreased (1/4x) ionic strength salinity conditions. These findings serve as evidence for environmental controls on cell wall exteriors, and provide a mechanism for cell surface nucleation in environments in which low temperature dolomite forms.

References

Beveridge, T. J., and L. L. Graham, 1991, Surface layers of bacteria, Journal of Microbiology, Rev. 55, p. 684–705.

Borrok, D., Turner, B. F., & Fein, J. B., 2005, A universal surface complexation framework for modeling proton binding onto bacterial surfaces in geologic settings. *American Journal of Science*, v. 305, n. 6, p. 826-853.

Braissant, O., Decho, A. W., Dupraz, C., Glunk, C., Przekop, K. M., & Visscher, P. T., 2007, Exopolymeric substances of sulfate-reducing bacteria: Interactions with calcium at alkaline pH and implication for formation of carbonate minerals, *Geobiology*, v. 5, n. 4, p. 401-411.

Cunningham, A. F., & Spreadbury, C. L., 1998, Mycobacterial stationary phase induced by low oxygen tension: cell wall thickening and localization of the 16-kilodalton α-crystallin homolog. *Journal of bacteriology*, v. 180, n. 4, p. 801-808.

Daughney, C. J., Feinf, J. B., & Yee, N., 1998, A comparison of the thermodynamics of metal adsorption onto two common bacteria. *Chemical Geology*, v. 144, n. 3, p. 161-176.

Dawson, K. S., Freeman, K. H., & Macalady, J. L., 2012, Molecular characterization of core lipids from halophilic archaea grown under different salinity conditions, *Organic Geochemistry*, v. 48, p. 1-8.

Elshahed, M. S., Savage, K. N., Oren, A., Gutierrez, M. C., Ventosa, A., & Krumholz, L. R., 2004, Haloferax sulfurifontis sp. nov., a halophilic archaeon isolated from a sulfide-and sulfur-rich spring. International journal of systematic and evolutionary microbiology, v. 54, n. 6, p. 2275-2279.

Fein, J. B., Daughney, C. J., Yee, N., & Davis, T. A., 1997, A chemical equilibrium model for metal adsorption onto bacterial surfaces. *Geochimica et Cosmochimica Acta*, v. 61, n. 16, p. 3319-3328.

Kenward, P. A., Fowle, D. A., Goldstein, R. H., Ueshima, M., González, L. A., & Roberts, J. A. (2013). Ordered low-temperature dolomite mediated by carboxyl-group density of microbial cell walls. AAPG bulletin, v. 97, n. 11, p. 2113-2125.

Kinnebrew, N., 2012, Surface sorption properties of halophilic Archaea: Master's thesis, University of Kansas, Lawrence, Kansas, 50 p.

Müller, D. W., McKenzie, J. A., & Mueller, P. A., 1990, Abu Dhabi sabkha, Persian Gulf, revisited: application of strontium isotopes to test an early dolomitization model. *Geology*, v. 18, n. 7, p. 618-621.

Obuekwe, C. O., 1980, Ph.D. dissertation. University of Alberta, Edmonton, Alberta, Canada.

Oren, A., 1999, Bioenergetic aspects of halophilism. Microbiology and Molecular Biology Reviews, v. 63, p. 334–348.

Phoenix, V. R., Martinez, R. E., Konhauser, K. O., & Ferris, F. G., 2002, Characterization and implications of the cell surface reactivity of Calothrix sp. strain KC97. *Applied and environmental microbiology*, v. 68, n. 10, p. 4827-4834.

Phoenix, V. R., D. G. Adams, and K. O. Konhauser, 2000, Cyanobacterial viability during hydrothermal biomineralization. Chem. Geol. v. 169, p. 329–338.

Roberts, J. A., Kenward, P. A., Fowle, D. A., Goldstein, R. H., González, L. A., & Moore, D. S., 2013, Surface chemistry allows for abiotic precipitation of dolomite at low temperature, *Proceedings of the National Academy of Sciences*. v. 110, n. 36, p. 14540-14545.

Sára, M., & Sleytr, U. B., 2000, S-layer proteins. Journal of bacteriology, v. 182, n. 4, p. 859-868.

Shockman, G. D., 1965, Symposium on the fine structure and replication of bacteria and their parts. IV. Unbalanced cell-wall synthesis: autolysis and cell-wall thickening. *Bacteriological reviews*, v. 29, n. 3, p. 345.

Turner, B. F., & Fein, J. B., 2006, Protofit: a program for determining surface protonation constants from titration data. Computers & geosciences, v. 32, n. 9, p. 1344-1356.

Van Houte, J., & Saxton, C. A., 1971, Cell wall thickening and intracellular polysaccharide in microorganisms of the dental plaque. *Caries research*, v. 5, n.1, p. 30-43.

Warthmann, R., van Lith, Y., Vasconcelos, C., McKenzie, J. A., & Karpoff, A. M., 2000, Bacterially induced dolomite precipitation in anoxic culture experiments. *Geology*, v. 28, n. 12, p. 1091-1094.

Warthmann, R., Vasconcelos, C., Sass, H., & McKenzie, J. A., 2005, Desulfovibrio brasiliensis sp. nov., a moderate halophilic sulfate-reducing bacterium from Lagoa Vermelha (Brazil) mediating dolomite formation. *Extremophiles*, v. 9, n. 3, p. 255-261.

Warren, J. K., 1990, Sedimentology and mineralogy of dolomitic Coorong lakes, South Australia. *Journal of Sedimentary Research*, v. 60, n. 6.

Yu, W., Dodds, W.K., Banks, M.K., Skalsky, J., and Strauss, E.A., 1995. Optimal staining and sample storage time for direct microscopic enumeration of total and active bacteria in soil with two fluorescent dyes. *Applied and Environmental Microbiology*, v. 61, n. 9, p. 3367-3372.

Chapter 3: Geologic Implications

This research extends previous research completed on the cell walls of microorganisms by measuring changes in functional group density, when grown in a variety of salinities (Borrok et al., 2005). The findings of this research have shown that microorganisms can rapidly modify their exteriors to survive harsh large changes in solution salinity, and, in turn, foster the necessary conditions that may elicit nucleation points for low temperature dolomite precipitation.

Data collected in this research provide a plausible explanation for why dolomite forms where it does (i.e. sabkha, mixing zones, hypersaline lagoons). The geochemical conditions must be favorable, but biomass with the proper carboxyl group density (>0.06 carboxyl groups $Å^{-2}$) must also be present for to serve as nucleation sites for dolomite templates to form.

This research provides opportunities for additional studies investigating cell wall modification that occur with other microorganisms associated with low temperature dolomite precipitation (including, but not limited to *Virgibacillus marismortui* and *Marinobacter sp, Desulfobulbus mediterraneus,* etc.). These additional studies could confirm increased carboxyl group density among various microorganisms to show environmental influence on cell wall structure and function. Additionally, studies that utilize native microbial communities, rather than pure cultures, will further elucidate the role that microorganisms play in low temperature dolomite formation.

Beyond its relation to low temperature dolomite precipitation, this research has practical applications for metal bioremediation in aqueous environments. These microorganisms could be engineered to maximize surface functional groups, allowing ventures

in bioremediation to successfully (and efficiently) bioaugment soil and groundwater systems (Vogel, 1995; Fantroussi & Agathos, 2005) to adsorb free cations, such as lead, cadmium, zinc, cobalt, nickel, chromium, aluminum that are then extracted with the cations still attached. Perhaps this division of bio-engineering (Pieper & Reineke, 2000; Sayler & Ripp, 2000) will solve problems of ecosystem contamination that were once deemed impossible to remedy.

Additional applications include the injection of polystyrene spheres (covered with carboxyl groups), acting as surrogate microorganisms, or engineered biomass into the subsurface, providing necessary nucleation points for dolomite formation. These techniques would be appropriate to sequester heavy metals in dolomite, a phase that is less soluble than calcite the mineral typically used for radionuclide/heavy metal sequestration in the subsurface (White et al., 1995; Knox et al., 2003). Furthermore, CO_2 sequestration in dolomite would be an attractive long term storage solution in deep saline aquifers targeted for CCUS (carbon capture and underground storage) (Anderson & Newell, 2004; Azar et al., 2006) . Additional research in these areas are necessary to initiate these engineering endeavors.

References

Anderson, S., & Newell, R., 2004, Prospects for carbon capture and storage technologies. *Annu. Rev. Environ. Resour.*, v. 29, p. 109-142.

Azar, C., Lindgren, K., Larson, E., & Möllersten, K., 2006, Carbon capture and storage from fossil fuels and biomass–Costs and potential role in stabilizing the atmosphere. *Climatic Change*, v. 74, n. 1-3, p. 47-79.

Borrok, D., Turner, B. F., & Fein, J. B., 2005, A universal surface complexation framework for modeling proton binding onto bacterial surfaces in geologic settings. *American Journal of Science*, v. 305, n. 6, p. 826-853.

El Fantroussi, S., & Agathos, S. N., 2005, Is bioaugmentation a feasible strategy for pollutant removal and site remediation?. *Current opinion in microbiology*, v. 8, n. 3, p. 268-275.

Knox, A. S., Kaplan, D. I., Adriano, D. C., Hinton, T. G., & Wilson, M. D., 2003, Apatite and phillipsite as sequestering agents for metals and radionuclides. *Journal of environmental quality*, v. 32, n. 2, p. 515-525.

Pieper, D. H., & Reineke, W., 2000, Engineering bacteria for bioremediation. *Current Opinion in Biotechnology*, v. 11, n. 3, p. 262-270.

Sayler, G. S., & Ripp, S., 2000, Field applications of genetically engineered microorganisms for bioremediation processes. *Current Opinion in Biotechnology*, v. 11, n. 3, p. 286-289.

Vogel, T. M., 1996, Bioaugmentation as a soil bioremediation approach. *Current opinion in biotechnology*, v. 7, n. 3, p. 311-316.

White, C., Wilkinson, S. C., & Gadd, G. M., 1995, The role of microorganisms in biosorption of toxic metals and radionuclides. *International Biodeterioration & Biodegradation*, v. 35, n. 1, p.17-40.

Appendix: Tables and Figures

Table 1: Morphological, metabolic, and incubation differences between the microorganisms of study

Microorganism	*Desulfovibrio brasiliensis*	*Shewanella putrefaciens*	*Haloferax sulfurifontis*
Domain	Bacteria	Bacteria	Archaea
Strain Designation	LVform1 (DSM# 15816)	200R (ATCC® 51753™)	M6 (ATCC® BAA-897™)
Oxygen Tolerance	Anaerobe	Facultative Anaerobe	Aerobe
Metabolism	Sulfate Reduction	Iron & Manganese Reduction	Sulfur Oxidation
Shape	Vibrio	Rod	Rods, Flattened Discs, and Irregular
Size (µm, width X length)	0.30-0.45 X 1.0-3.5 (Warthmann, 2005)	0.5-1.0 X 2.0-5.0 (Sokolov et al., 2001)	0.5-0.6 X 1.5-1.7 (Elshahed, et al., 2004)
Calculated Surface Area Per Microbial Cell	5.58 μm^2 High 3.09 μm^2 Medium 1.23 μm^2 Low	18.85 μm^2 High 10.01 μm^2 Medium 3.93 μm^2 Low	1.88 μm^2 High 1.62 μm^2 Medium 1.37 μm^2 Low
Cell Density	1.27 x 10^8 cells/mL	6.8 x 10^8 cells/mL	5.0 x 10^8 cells/mL
Color (in Liquids)	White/Translucent	Bright Pink	Red
Gram Type	Negative	Negative	Negative
Isolation Location	Lagoa Vermelha, Rio de Janeiro, Brazil	Alberta, Canada	Oklahoma, USA
Isolation Environment	Hypersaline Lagoon	Oil Pipeline	Microbial Mat in a Sulfur Spring
Carboxyl Group Density (from literature)	1.64−2.39 mol/kg (EPS) (Braissant et al., 2007)	0.45 mol/kg (Sokolov et al., 2001)	1.6 mol/kg (Kinnebrew, 2012)
Growth Temperature	30-33°C	30°C	35-37°C
pH Growth Range	6.3-9.0	7.4-8.6	6.5-7.5
Salinity Growth Range	0.15-1.1 M NaCl	0.1-3.0 M NaCl	0.3-2.6 M NaCl
Liquid Media	DSMZ Medium 383	ATCC® Medium 18	ATCC® Medium 2448
Mid-Exponential Growth Incubation Period	2.0-2.5 Days	4-5 Hours	6-8 Hours

Table 2: DSMZ *Desulfovibrio brasiliensis* media recipe for creating 0.5 M ionic strength media

DSMZ Recipe 383 Desulfobacterium Medium			
Solution A: Salts	0.5 M	1.0 M	1.5 M
Na_2SO_4	3 g	6 g	9 g
KH_2PO_4	0.2 g	0.4 g	0.6 g
NH_4Cl	0.3 g	0.6 g	0.9 g
NaCl	21 g	42 g	63 g
$MgCl_2$ x 6 H_2O	3 g	6 g	9 g
KCl	0.5 g	1.0 g	1.5 g
$CaCl_2$ x 2 H_2O	0.15 g	0.3 g	0.45 g
Resazurin	1 mg	--	--
Distilled water	930 ml	--	--

Solution B: Trace elements SL-10 (Med 320)		
HCl (25%; 7.7 M)	10 ml	
$FeCl_2$ x 4 H_2O	1.5 g	
$ZnCl_2$	70 mg	
$MnCl_2$ x 4 H_2O	100 mg	
H_3BO_3	6 mg	
$CoCl_2$ x 6 H_2O	190 mg	
$CuCl_2$ x 2 H_2O	2 mg	
$NiCl_2$ x 6 H_2O	24 mg	
Na_2MoO_4 x 2 H_2O	36 mg	
Distilled water	990 ml	

Only use 1.00 ml for final media solution. First dissolve $FeCl_2$ in the HCl, then dilute in water, add and dissolve the other salts. Finally make up to 1000.0 ml.

Solution C: Sodium Bicarbonate	
$NaHCO_3$	2.5 g
Distilled water	50 ml

Solution D: Substrate	
Na-L-lactate	2.3 g
Distilled water	10 mL

Solution E: Vitamin solution (Med 141)	
Biotin	2 mg
Folic acid	2 mg
Pyridoxine-HCl	10 mg
Thiamine-HCl x 2 H_2O	5 mg
Riboflavin	5 mg
Nicotinic acid	5 mg
D-Ca-pantothenate	5 mg
Vitamin B12	0.1 mg
p-Aminobenzoic acid	5 mg
Lipoic acid	5 mg

Only use 10.00 ml for final media solution.

Solution F: Sodium Selenate	
Na_2SeO_3 x 5 H_2O-sol	(3 mg in 0.01 M NaOH) 1 ml

Solution G: Sodium Sulfide Nonahydrate	
Na_2S x 9 H_2O	0.4 g
Distilled water	10 ml

Solution A is prepared and autoclaved anoxically under 80% N_2 + 20% CO_2 gas atmosphere. Solution C is filter-sterilized and gassed for 20 min with 80% N_2 + 20% CO_2 gas mixture. Solutions B, D, E and F are filter-sterilized and gassed with 100% N_2. Solution G is autoclaved under 100% N_2. Solutions B to G are added to the sterile, cooled solution A in the sequence as indicated. Final pH of the medium should be 7.0. Addition of 10 - 20 mg sodium dithionite per liter (e.g. from 5% (w/v) solution freshly prepared under N_2 and filter-sterilized) may stimulate growth of all strains at the beginning. For transfers use 5 - 10% inoculum. Incubate all strains in the dark.

Table 3: *Shewanella putrefaciens* media recipe for creating various ionic strength media

ATCC® *S. putrefaciens*	**0.1 M IS**	**1.0 M IS**	**2.0 M IS**	**3.0 M IS**
BD™ Trypticase™ Soy Broth	30 g/L	--	--	--
Pancreatic Digest of Casein	(17 g)	--	--	--
Papaic Digest of Soybean	(3 g)	--	--	--
NaCl	(5 g)	+ 50.9 g	+ 109.4 g	+167.9 g
K_2HPO_4	(2.5 g)	--	--	--
$C_6H_{12}O_6$	(2.5 g)	--	--	--
Distilled Water	1,000 mL	--	--	--

Table 4: *Haloferax sulfurifontis* media recipe for creating various ionic strength media

ATCC® *H. sulfurifontis* Medium 2448	**3.2 M IS**	**1.6 M IS**	**0.8 M IS**	**0.4 M IS**	**0.2 M IS**
NaCl	150 g	75 g	37.5 g	18.75 g	9.375 g
$MgCl_2$	20 g	21.35 g	10.675 g	5.3375 g	2.66875 g
K_2SO_4	0.5 g	0.25 g	0.125 g	0.0625 g	0.03125 g
$CaCl_2 \times H_2O$	0.1 g	0.066 g	0.033 g	0.0165 g	0.00825 g
Yeast Extract	5 g	--	--	--	--
Distilled Water	1 L	--	--	--	--

Table 5: Optimal ionic strength growth conditions and experimental trial conditions.

Microorganism	**Optimal Ionic Strength Conditions for Growth (M)**	**Experimental Ionic Strength Trials (M)**					
Desulfovibrio brasiliensis	0.5	0.2	0.3	0.4	0.6	1.0	1.5
Shewanella putrefaciens	0.1	1.0	2.0	3.0	--	--	--
Haloferax sulfurifontis	3.2	1.6	1.0	0.8	0.4	0.2	--

Table 6: Microorganism ProtoFit Data Outputs: Calculated Acid Dissociation Constant (pK_a), Initial (Optimal) & Experimental Trial Site Density (SD), and Total Site Density

Desulfovibrio brasiliensis	Site 1*	Site 2	Site 3	Total Site Density
pK_a	4.58 ± 0.11	6.09 ± 0.08	7.61 ± 0.11	
Initial SD (kg/mol) 0.5 M Ionic Strength	0.09 ± 0.01	0.08 ± 0.01	0.09 ± 0.01	0.27 ± 0.02
Trial SD (kg/mol) 1.0 M Ionic Strength	0.26 ± 0.01	0.16 ± 0.01	0.19 ± 0.05	0.6 ± 0.07

Shewanella putrefaciens	Site 1	Site 2*	Site 3	Site 4	Total Site Density
pK_a	3.86 ± 0.20	5.09 ± 0.22	6.65 ± 0.17	8.19 ± 0.13	
Initial SD (kg/mol) 0.1 M Ionic Strength	0.31 ± 0.01	0.13 ± 0.01	0.22 ± 0.04	0.23 ± 0.04	0.88 ± 0.06
Trial SD (kg/mol) 2.0 M Ionic Strength	0.37 ± 0.03	0.22 ± 0.02	0.25 ± 0.02	0.37 ± 0.04	1.1 ± 0.1

Haloferax sulfurifontis	Site 1*	Site 2	Site 3	Total Site Density
pK_a	4.38 ± 0.14	5.98 ± 0.10	8.38 ± 0.16	
Initial SD (kg/mol) 3.2 M Ionic Strength	0.34 ± 0.04	0.18 ± 0.03	0.25 ± 0.05	0.77 ± 0.11
Trial SD (kg/mol) 0.8 M Ionic Strength	0.18 ± 0.04	0.09 ± 0.02	0.33 ± 0.1	0.6 ± 0.15

*Carboxyl group sites.

Table 7: Calculated range of microorganism surface area with high, medium, and low values

Microorganism	*Desulfovibrio brasiliensis*	*Shewanella putrefaciens*	*Haloferax sulfurifontis*
Range of calculated surface area per microorganism	5.58 μm^2 High 3.09 μm^2 Medium 1.23 μm^2 Low	18.85 μm^2 High 10.01 μm^2 Medium 3.93 μm^2 Low	1.88 μm^2 High 1.62 μm^2 Medium 1.37 μm^2 Low
Surface area value selected	3.09 μm^2 Medium	10.01 μm^2 Medium	1.62 μm^2 Medium

(Calculations with data from Braissant et al., 2007; Sokolov et al., 2001; & Elshahed, et al., 2004)

Table 8: Physico-Chemical Data for Studied Waters from Lagoa Vermelha and Surroundings

Samples	Temp (°C)	pH	Mg (mg/L)	Ca (mg/L)	Mg/Ca Ratio	Conductivity (mS)	Ionic Strength (M)
Lagoa Vermelha							
July 1991	23	8.2	975	330	2.95	43.00	0.70
August 1991	26	8.3	1,745	580	3.01	60.00	0.97
September 1991	24	8.0	1,400	455	3.07	51.00	0.83
October 1991	26	8.5	920	305	3.01	42.00	0.68
November 1991	27	8.1	540	170	3.17	27.30	0.44
December 1991	29	8.3	545	175	3.10	28.20	0.46
January 1992	28	8.1	400	130	3.07	24.20	0.39
February 1992	31	8.2	800	255	3.13	36.50	0.59
March 1992	29	8.3	680	230	2.95	34.00	0.55
April 1992	30	8.1	1,100	660	1.66	68.00	1.10
May 1992	32	8.3	2,200	870	2.52	78.00	1.27
June 1992	29	8.0	2,000	825	2.42	78.00	1.27
Other Nearby Waters							
Atlantic Ocean	22	--	1,590	620	2.56	42.00	0.68
Araruama (lagoon)	23	--	1,100	990	1.11	57.00	0.93
Jaconé (lagoon)	22	--	90	1,400	0.06	7.60	0.12
Jacarépia (lagoon)	22	--	131	1,010	0.13	2.30	0.04
Well	--	--	170	250	0.68	0.30	0.003

(Modified from Vasconcelos and McKenzie, 1997)

Table 9: Carboxyl Site Densities for Microorganisms and Exopolymeric Substances

Substrate	Carboxyl Site Concentration (mol g^{-1})	Carboxyl Site Density (Carboxyl $Å^{-2}$)	Mineral Precipitate
Bacillus subtilis	1.2×10^{-4} (Daughney et al., 2001)	0.01	No dolomite*
Shewanella putrefaciens	4.5×10^{-4} (Sokolov et al., 2001)	0.03	No dolomite*
Microspheres	1.4×10^{-4}*	0.02	No dolomite*
Methanobacterium formicicum	8.1×10^{-4}*	0.06	Disordered dolomite and Mg calcite*
Haloferax sulfurifontis	1.6×10^{-3} (Kinnebrew, 2012)	0.1	Ordered dolomite*
Exopolymeric substances (*Desulfovibrio sp.)*	1.6×10^{-3} - 2.4×10^{-3} (Braissant et al., 2007)	0.02-0.03	Disordered dolomite, Mg calcite, and Ca dolomite**
Exopolymeric substances (*Hymenobacter aerophilus)*	2.4×10^{-3} (Baker et al., 2010)	0.03	Unknown capacity
*Results from Kenward's research ** Results from Bontognali et al., 2008 and Vasconcelos et al., 2006			

(Reproduced from Kenward et al., 2013)

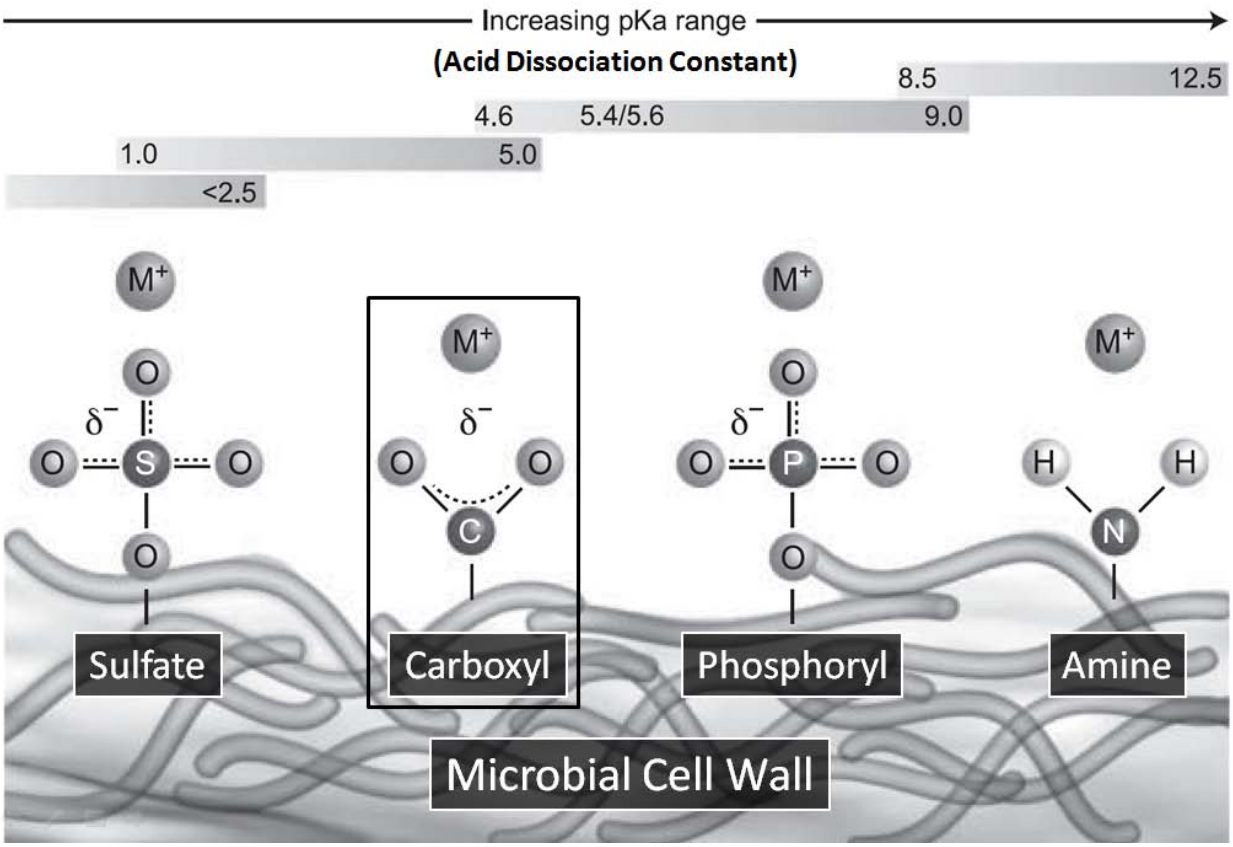

Figure 1: Diagram showing four common functional groups associated with exopolymeric substances (EPS), and theoretical interactions with positively-charged metals (M+). The listed pKa ranges for each functional group are indicated at the top of the figure.

(Modified from Braissant et al., 2007)

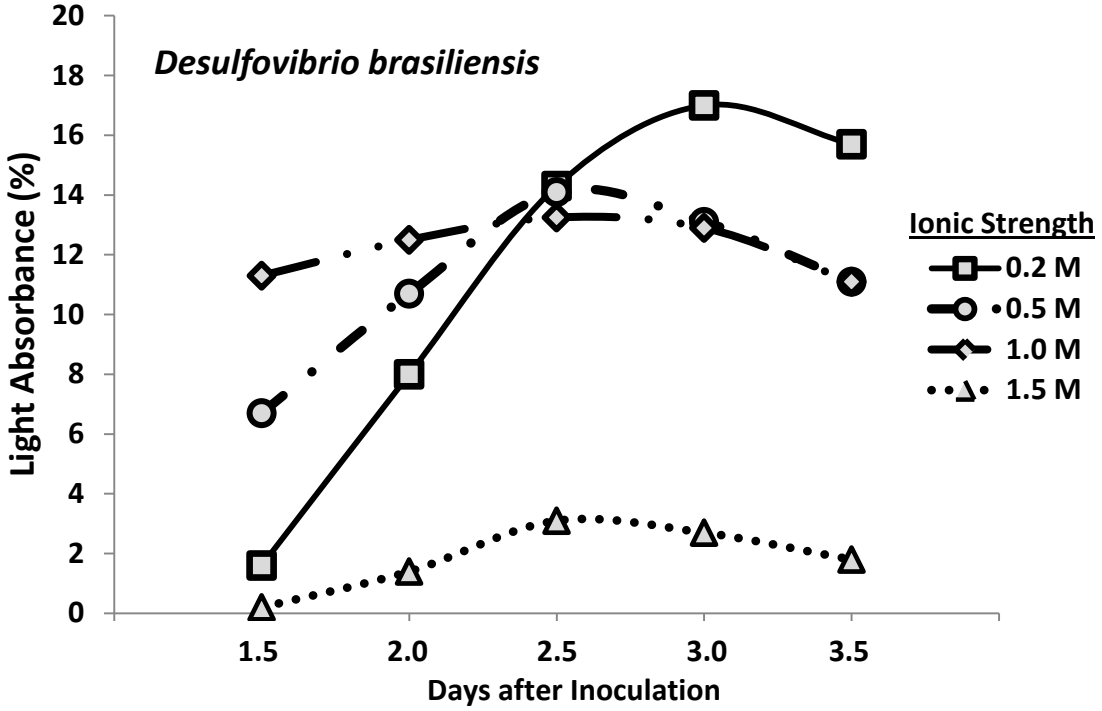

Figure 2: Growth curve of *Desulfovibrio brasiliensis* over 3.5 days. Mid-exponential growth was reached after 2.0 - 2.5 days for multiple growth conditions.

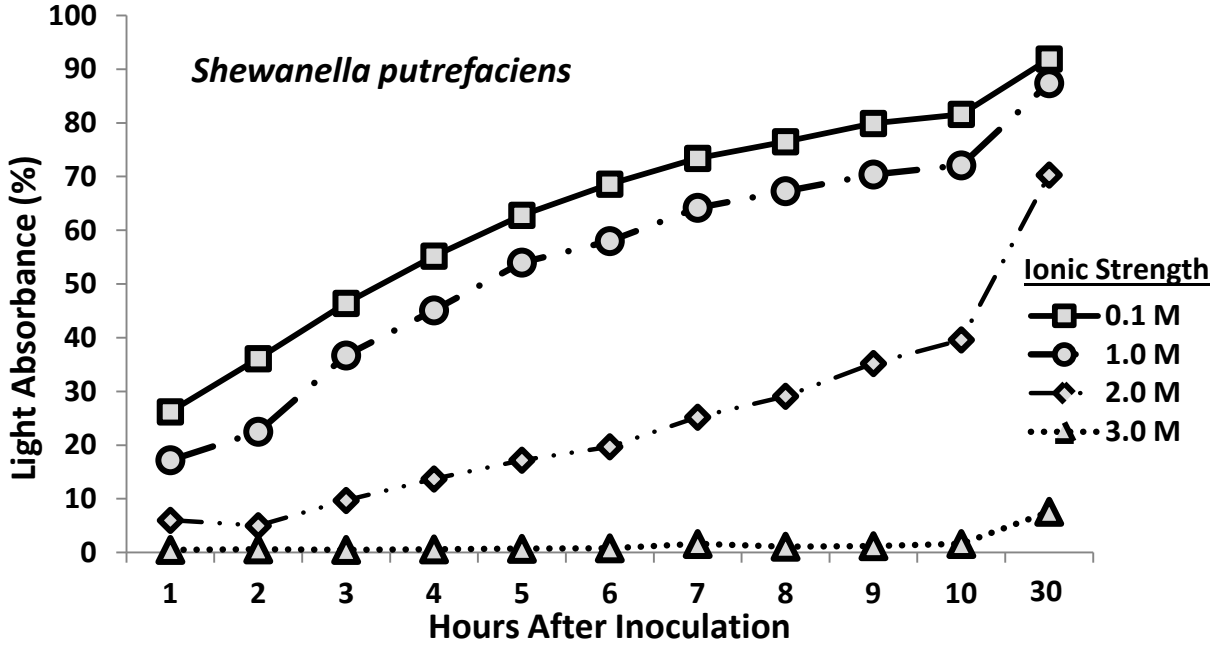

Figure 3: Growth curve of *Shewanella putrefaciens* over 30 hours. Mid-exponential growth was reached after approximately four hours for low ionic strength conditions.

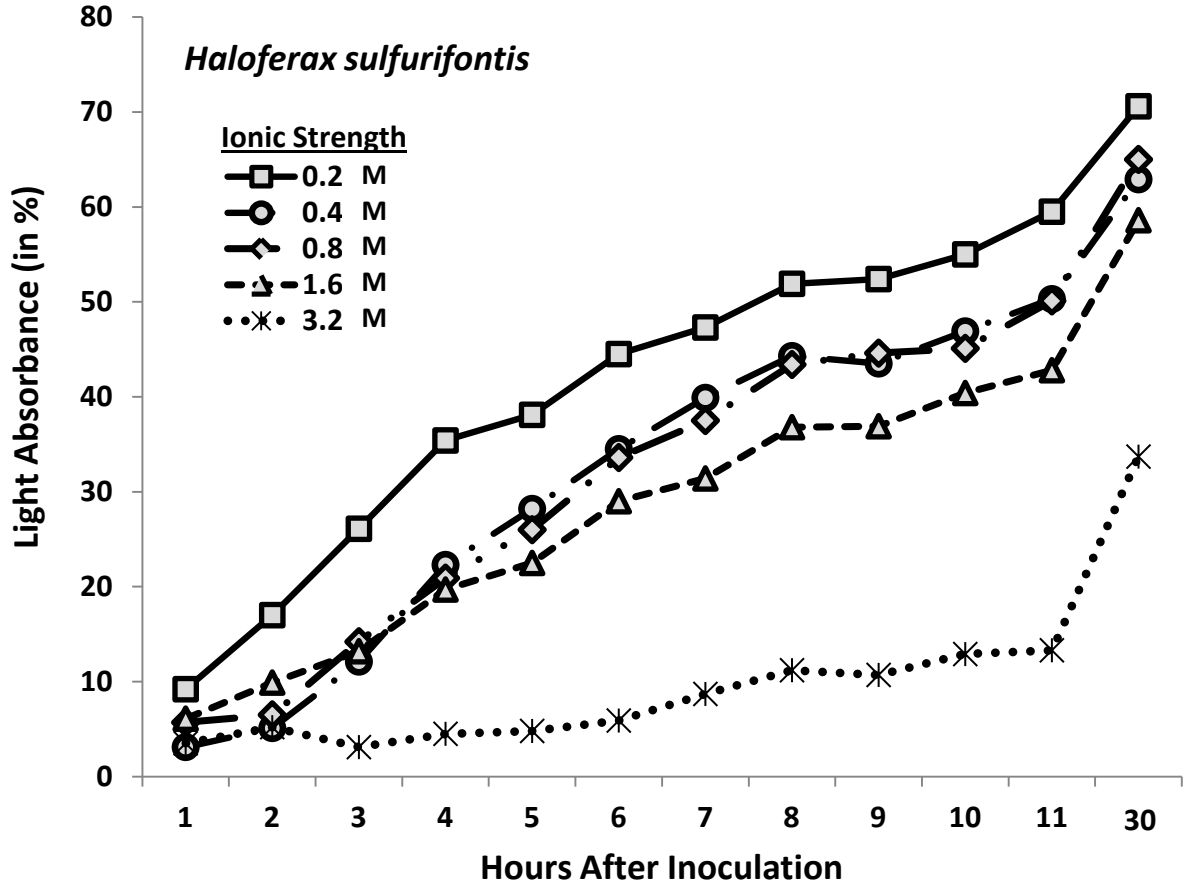

Figure 4: Growth curve of *Haloferax sulfurifontis* over 30 hours. Mid-exponential growth was reached after approximately 6-8 hours for low ionic strength conditions.

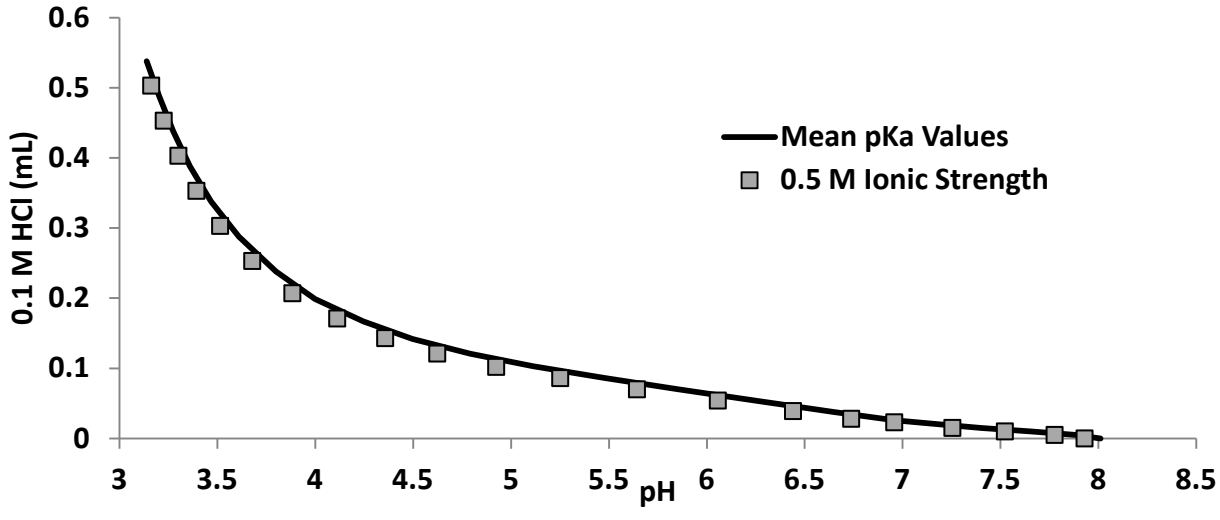

Figure 5: *Desulfovibrio brasiliensis* mean pKa value curve (generated by ProtoFit 2.1) and 0.5 M ionic strength acid titration curve.

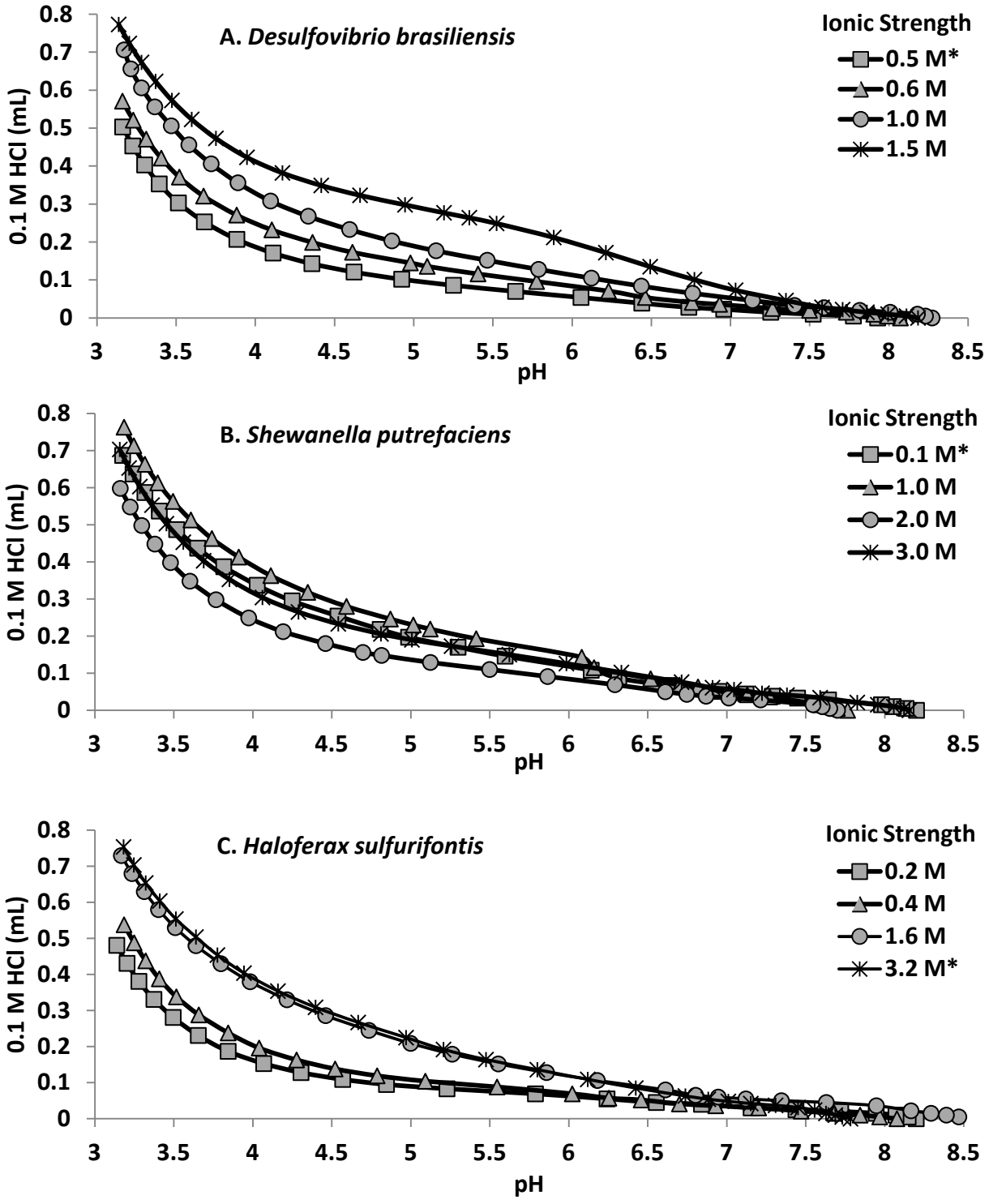

Figure 6: Acid titrations of microorganisms when grown in various ionic strengths with optimal growth conditions indicated by an asterisk (*). A. *D. brasiliensis*. B. *S. putrefaciens.* C. *H. sulfurifontis*.

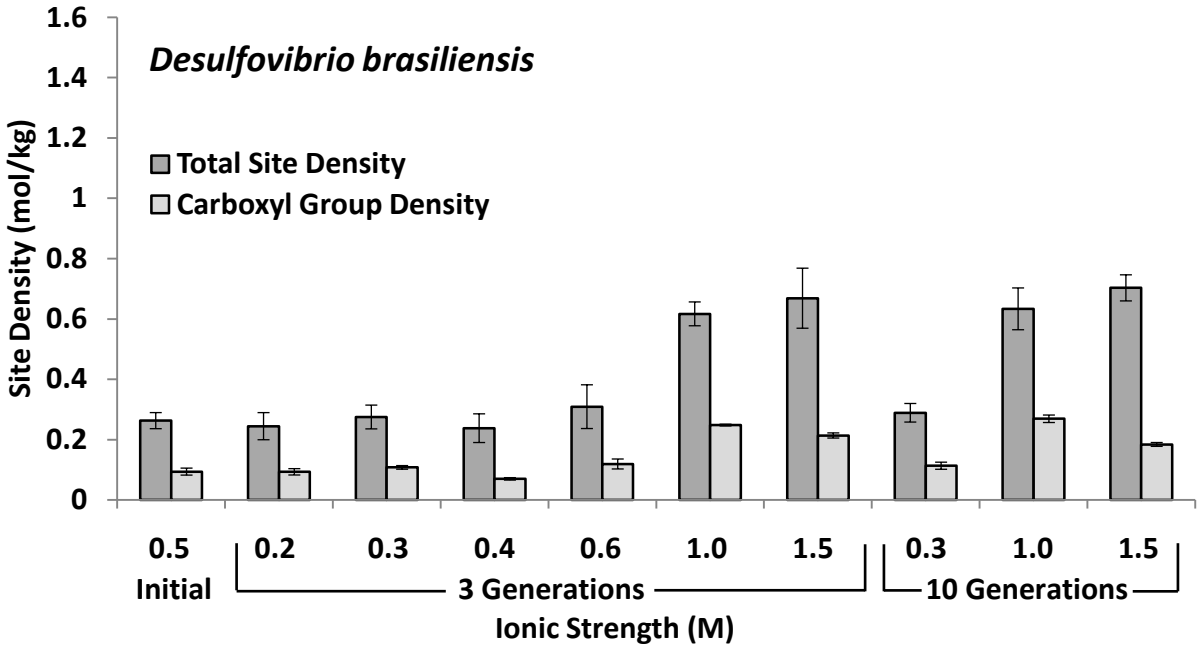

Figure 7: Carboxyl group density and total site density of *Desulfovibrio brasiliensis* after growth in various ionic strength conditions. A slight decrease in carboxyl group density occurs between 1.0 and 1.5 M ionic strength conditions.

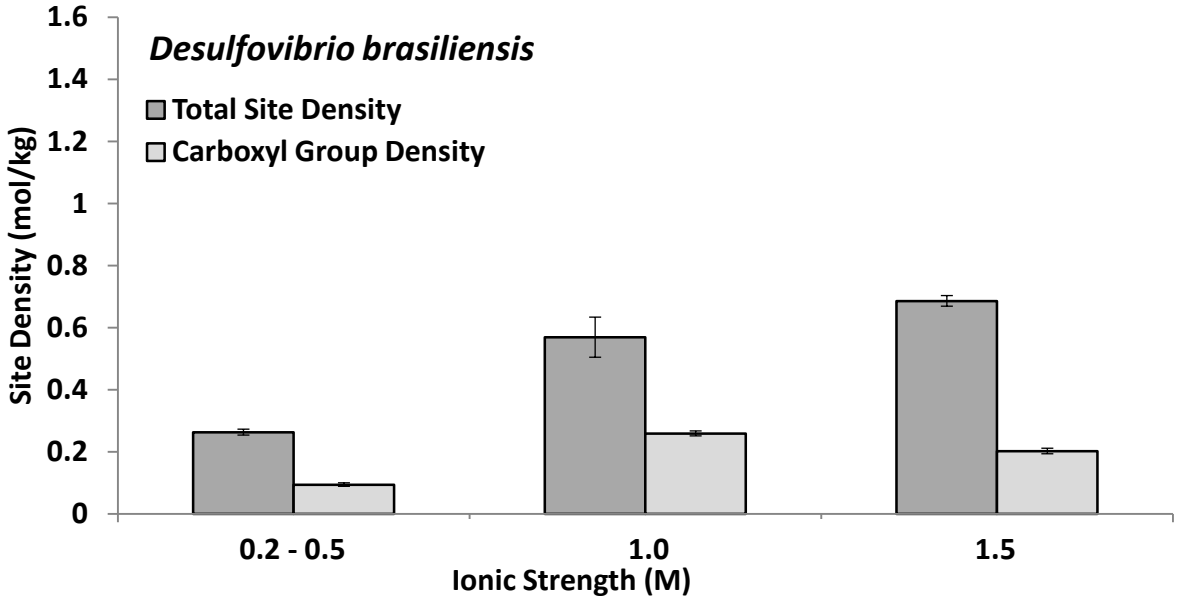

Figure 8: Summarized site densities for *D. brasiliensis*.

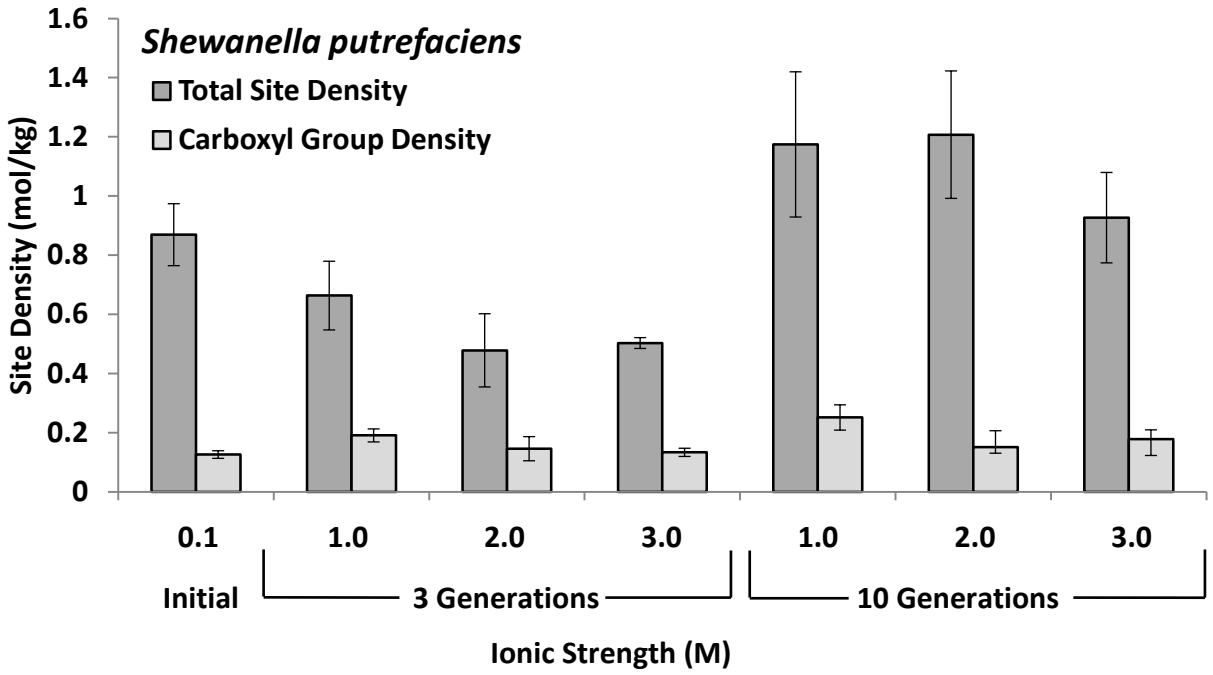

Figure 9: Carboxyl group density and total site density of *Shewanella putrefaciens* after growth in increased ionic strength conditions. A decrease in total site density occurs after three generations of growth in increased ionic strength conditions. After ten generations, an overall increase of total site density and carboxyl group density is measured.

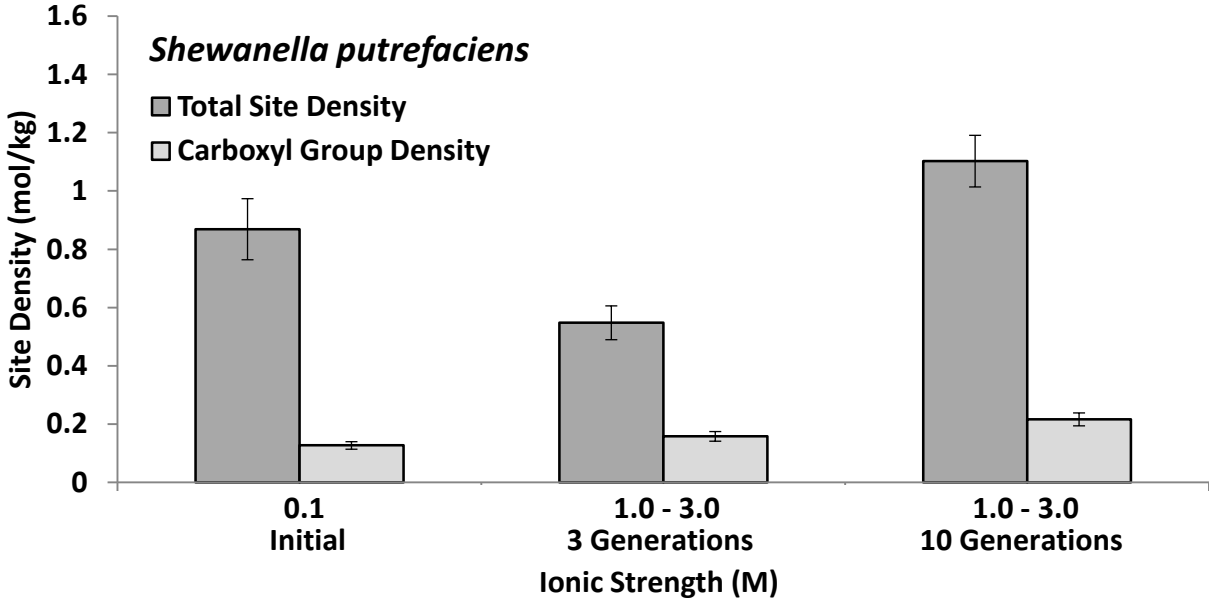

Figure 10: Summarized site densities for *S. putrefaciens* after multi-generational growth.

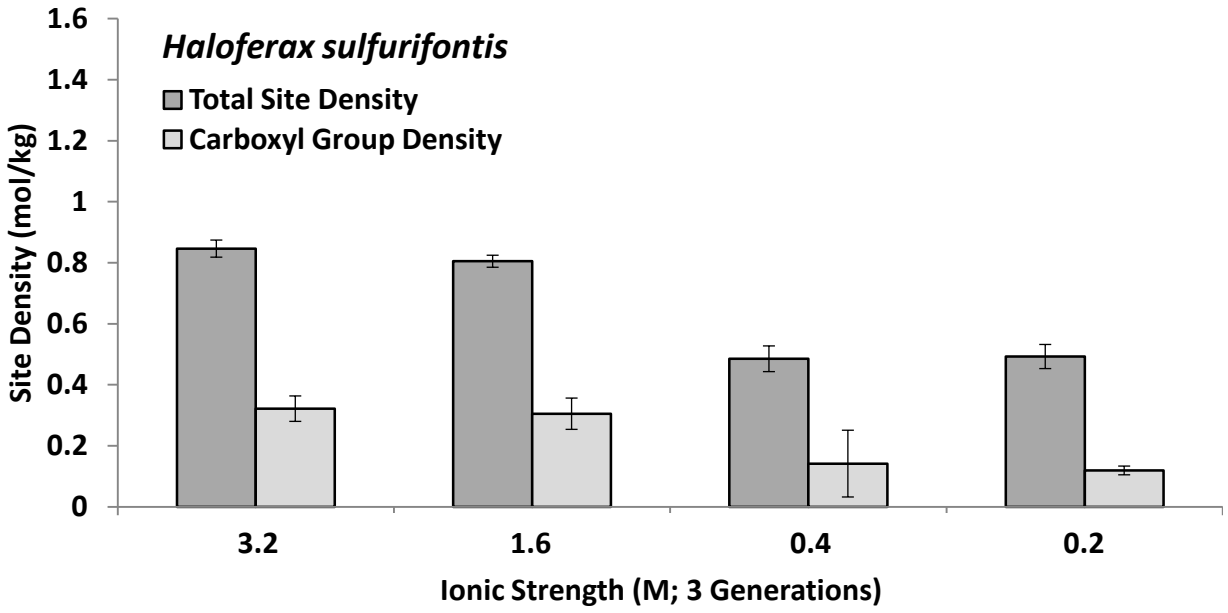

Figure 11: Carboxyl group density and total site density of *Haloferax sulfurifontis* after growth in decreased ionic strength conditions. A decrease in total site density and carboxyl group density occurs after three generations growth in decreased ionic strength conditions.

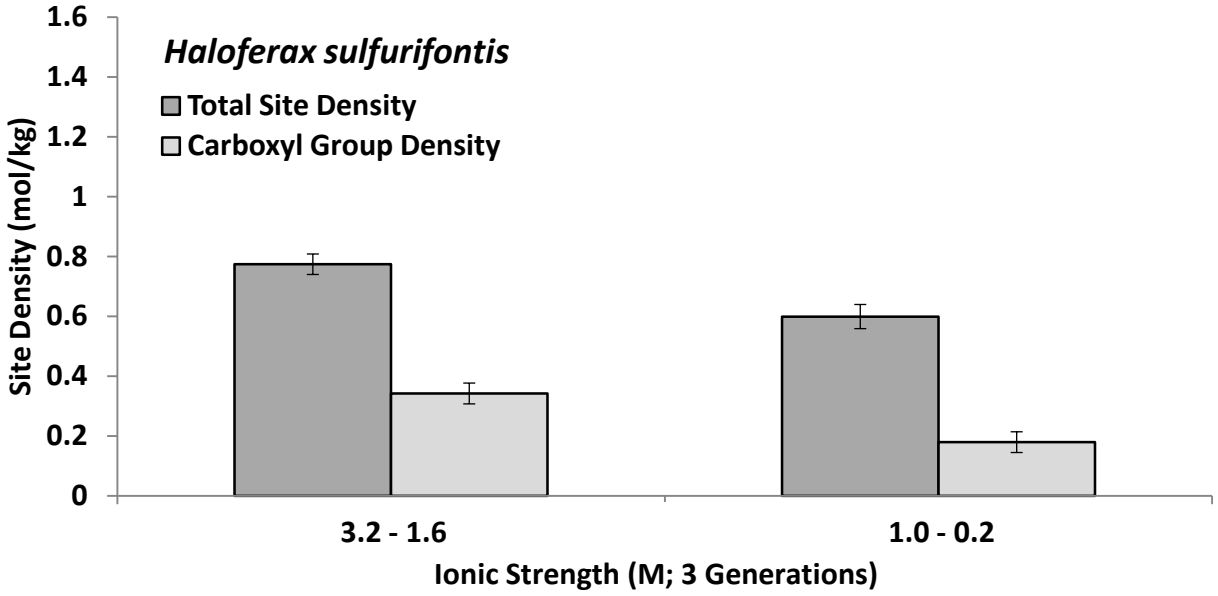

Figure 12: Summarized site densities for *H. sulfurifontis* after three generations of growth.

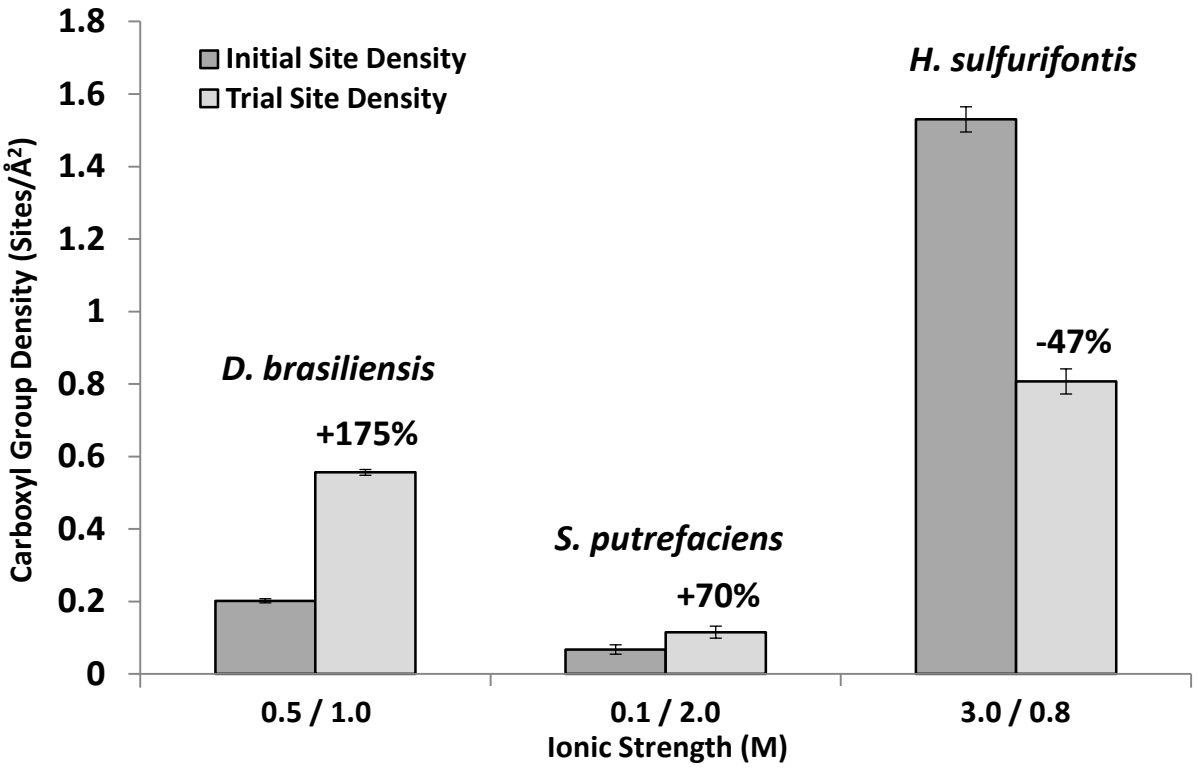

Figure 13: Carboxyl group density per $Å^2$ with measurements from both initial and experimental trials. *S. putrefaciens* has a relatively low carboxyl group density per $Å^2$, with an associated large relative cell size. Conversely, *H. sulfurifontis* has a relatively high carboxyl group density per $Å^2$, with an associated small relative cell size. *D. brasiliensis* also displays a relatively high carboxyl group density, when compared to *S. putrefaciens.*

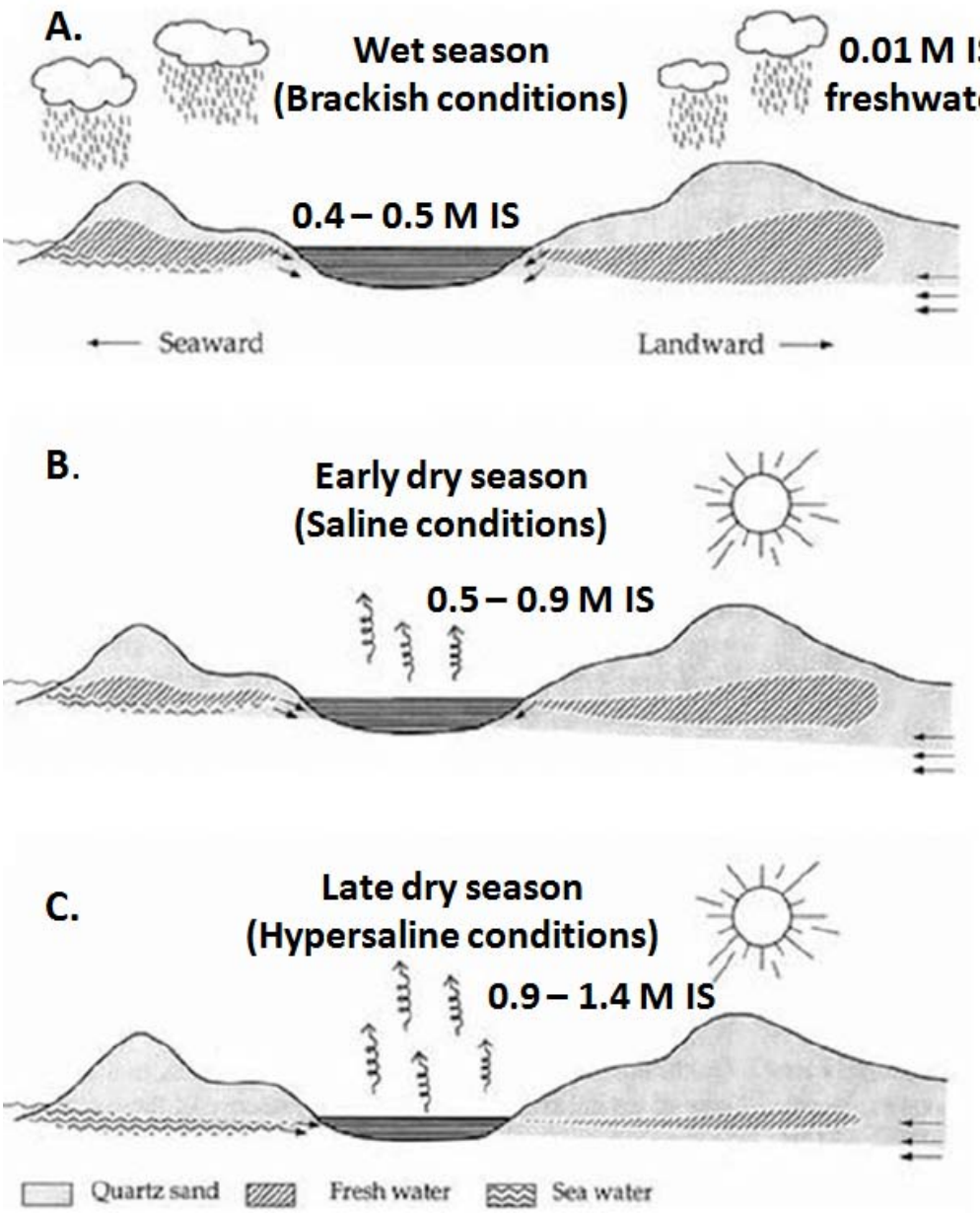

Figure 14: Schematic diagram showing various seasonality of *Lagoa Vermelha*. IS = Ionic Strength A. The increased rainfall during the wet season of *Lagoa Vermelha* produces brackish salinity conditions, as the water becomes dilute in dissolved ions. B. As the early dry season begins, rainfall becomes reduced, and salinity values increase to marine salinity. C. By the late dry season, all freshwater influx has ceased, and evaporation rates are at their peak, further increasing the ionic strength to hypersaline levels. Average marine ionic strength = 0.72 M.

(Figure modified from Vasconcelos & McKenzie, 1997)

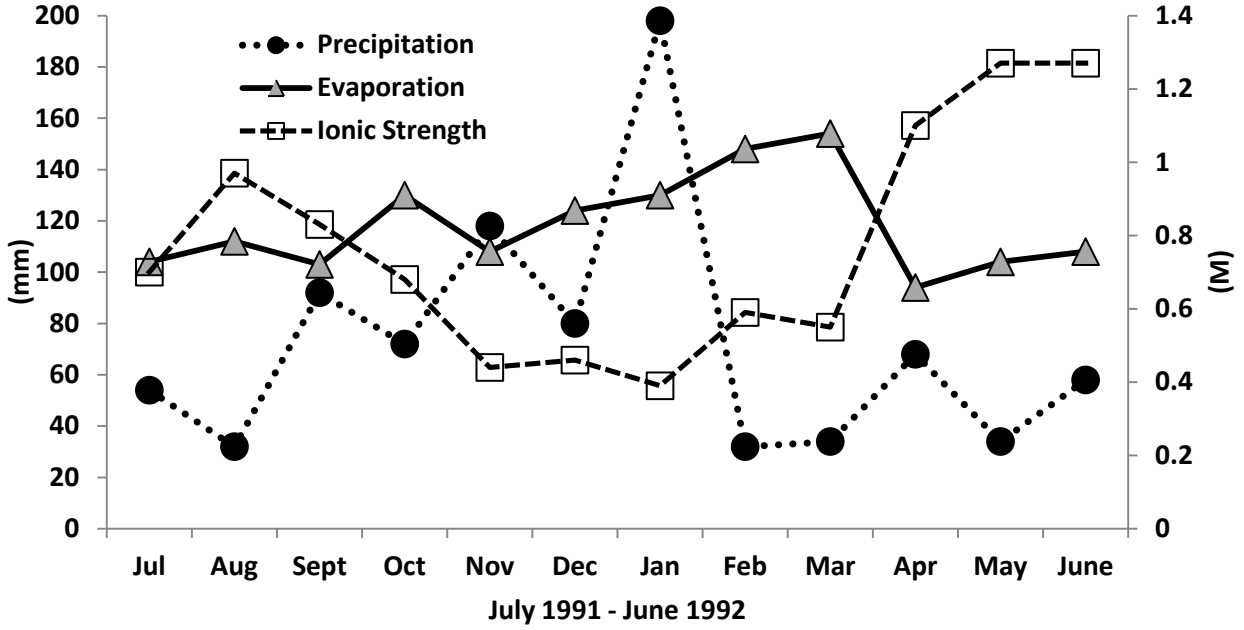

Figure 15: Lagoa Vermelha monthly evaporation and precipitation rates (in mm), and associated effect on ionic strength. (Figure modified from Vasconcelos and McKenzie, 1997.)

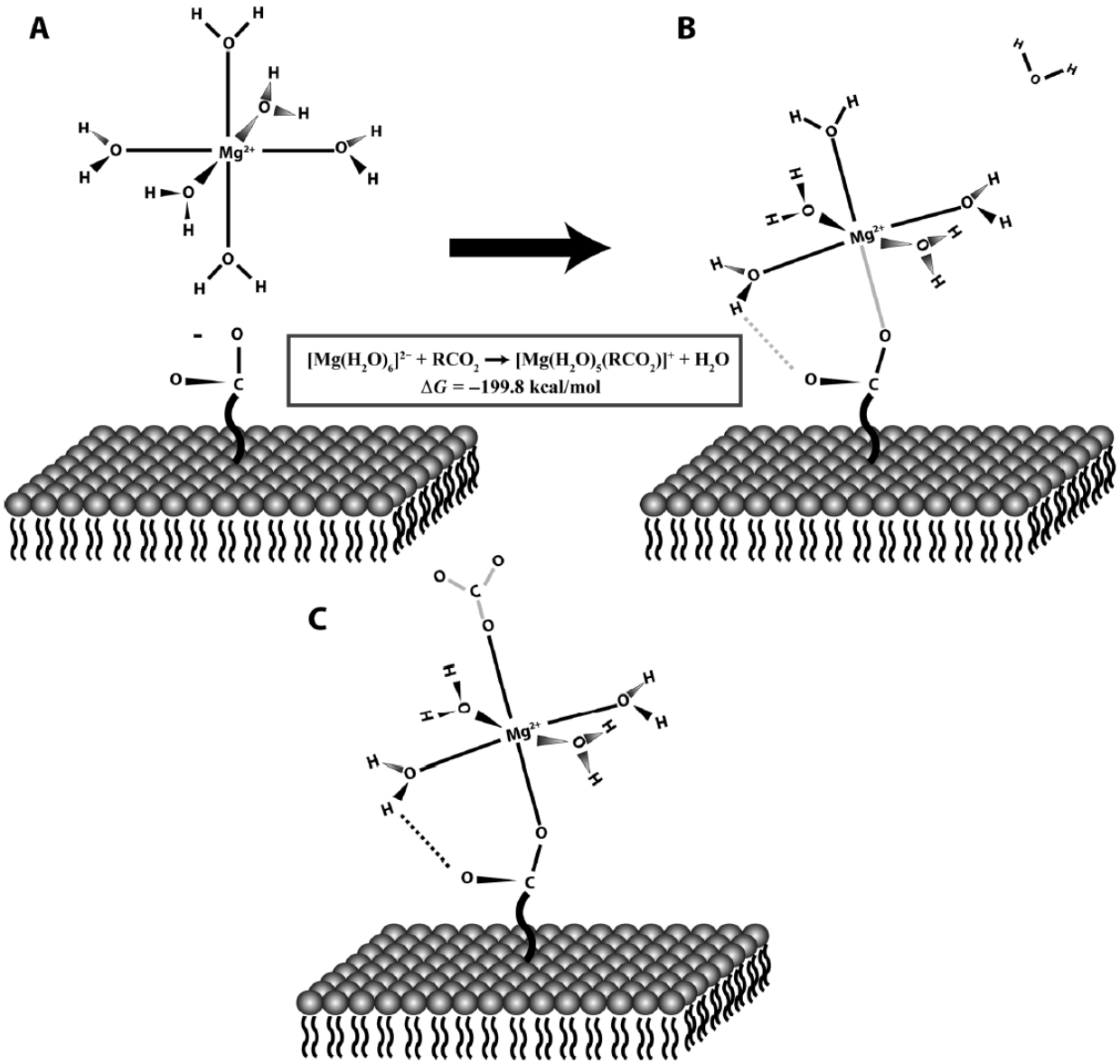

Figure 16: A: Displays behavior of the aqueous $[Mg(H_2O)_6]^{2+}$ with a negatively-charged carboxyl group (functional group) found on a microbial cell wall. The aqueous Mg^{2+} ion ejects a single molecule of H_2O, binding to the carboxyl group. B: Displays an energetically-favorable reaction (equation as shown). C: The new $[Mg(H_2O)_5(R\text{-}CO_2)]^+$ complex holds a positive charge that subsequently attract carbonate (CO_3^{2-}) or bicarbonate (HCO_3^{2-}) ions.

(Figure is reproduced from Kenward et al., 2013)

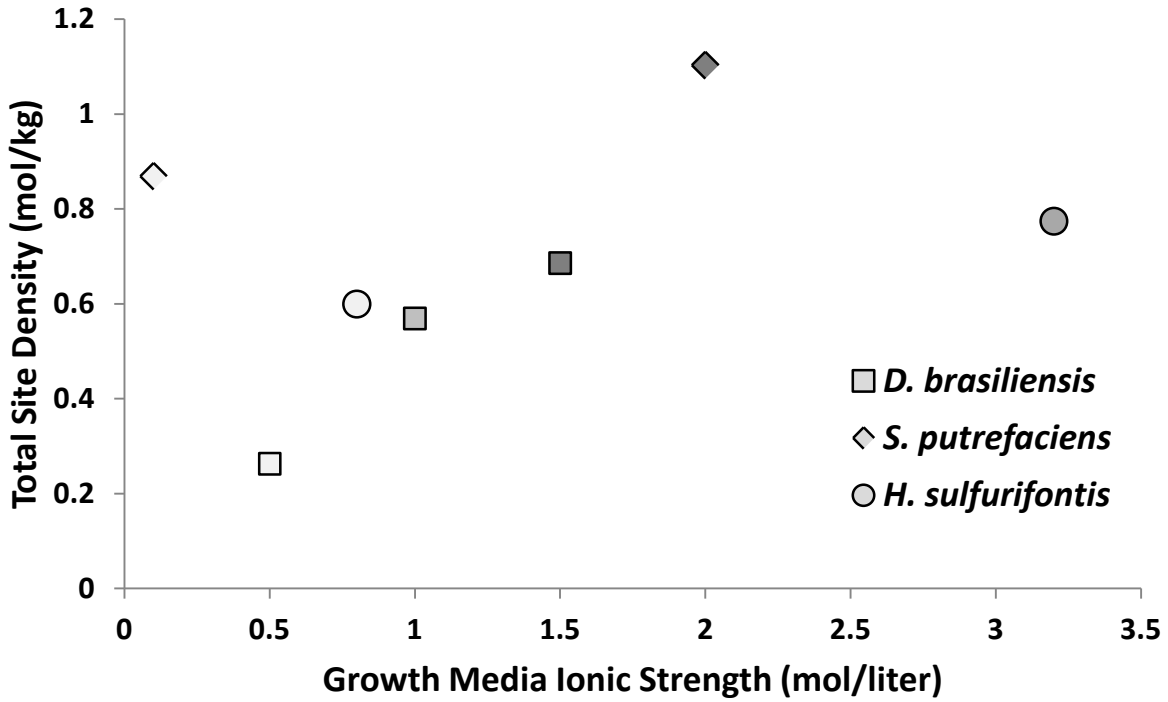

Figure 17: A plot of the total site density versus the growth media ionic strength. Lighter-filled markers indicate lower ionic strength growth media, while darker-filled markers indicate higher ionic strength growth media. A general trend is apparent: high ionic strength media correlates with increased total site density (carboxyl groups included).

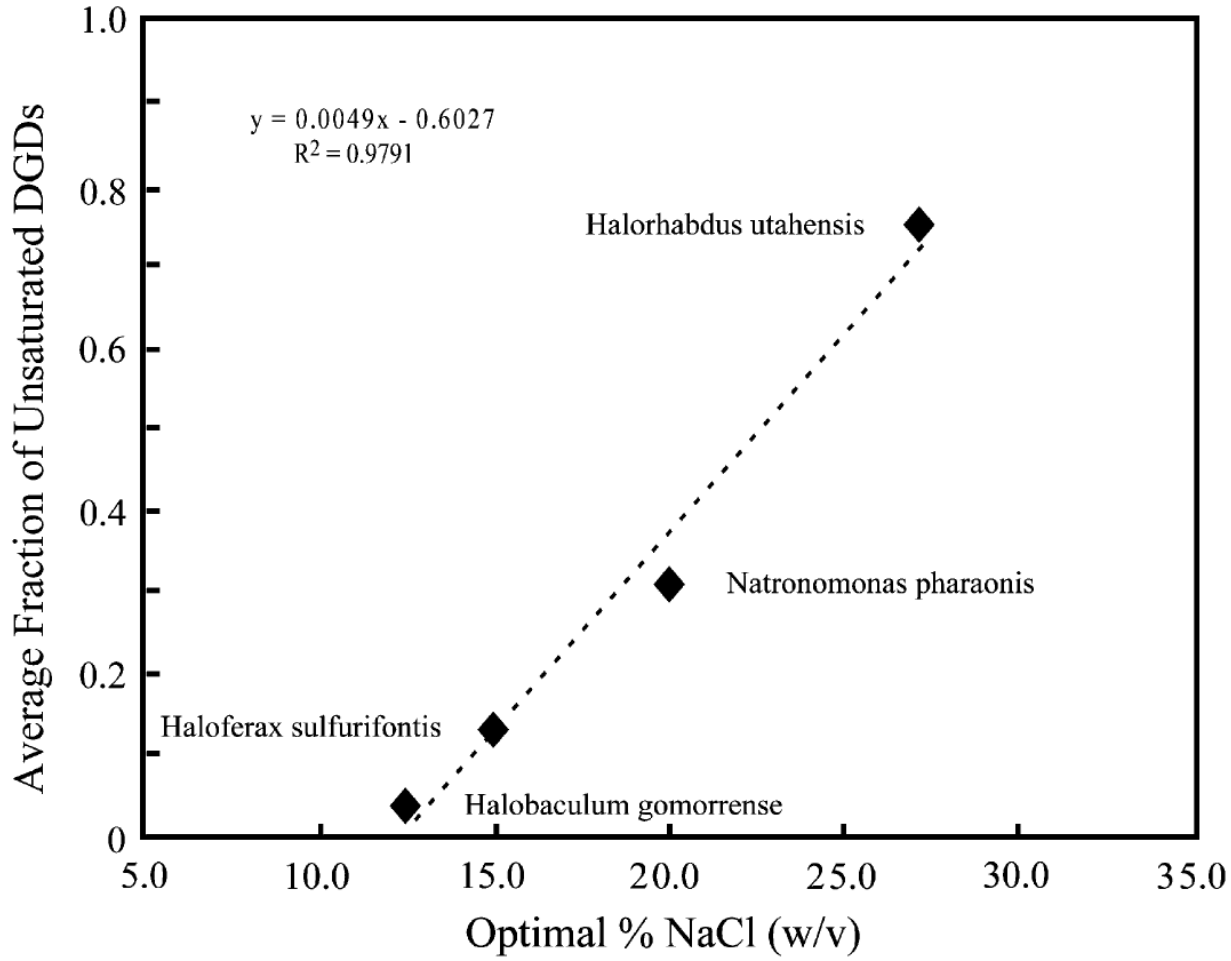

Figure 18: A plot of the average fraction of unsaturated DGDs vs. optimal % NaCl (w/v) for four different halophilic archaeal strains.

(Figure is reproduced from Dawson et al., 2002)